

Smart Sensor Shorts:

Prevention of hamstring injuries in professional and recreational football athletes by analyzing and monitoring kinematic data

S.S. Vinasithamby



Smart Sensor Shorts:

Prevention of hamstring injuries in professional and recreational football athletes by analyzing and monitoring kinematic data

by

S.S. Vinasithamby

in partial fulfilment of the requirements for the degree of

Master of Science
in BioMedical Engineering
specialisation Sports Engineering

at the Delft University of Technology,
to be defended publicly on Friday June 28, 2019 at 10:00 AM.

Student number:	4513770	
Thesis committee:	Prof. dr. F.C.T. van der Helm	TU Delft
	Ir. A.S.M. Steijlen	TU Delft
	Prof. dr. ir. K.M.B. Jansen	TU Delft
	Dr. D.J.J. Bregman	TU Delft
	Dr. E.A. Goedhart	KNVB

An electronic version of this thesis is available at <http://repository.tudelft.nl/>.

Preface

Hereby I present my Master Thesis to fulfill the requirements for the degree of Master of Science. The Master Thesis is the final result of my master in BioMedical Engineering at the TU Delft. The objective of the thesis was to develop a methodology to estimate the muscle strain and muscle elongation velocity of the hamstring muscles in professional and recreational football with the use of Inertial Measurement Units. This thesis consists of a scientific paper that describes the entire research study in a brief manner. Elaborations and background information regarding matters described in the scientific paper can be found in the appendices. This Master Thesis contains six appendices, each addressing a different topic.

- Appendix A; Detailed information about the process regarding the construction of the Smart Sensor Shorts.
- Appendix B; Detailed information about a small study that was performed regarding optimization of the kinematic data estimated with the use of the Smart Sensor Shorts.
- Appendix C; A concurrent validation study of the Smart Sensor Shorts compared with an Optoelectronic Motion Analysis System that was conducted during the internship at the KNVB SMC.
- Appendix D; The test protocol (written in Dutch) which was used by myself as researcher as guideline during the tests.
- Appendix E; The information letter (written in Dutch) that was sent to (potential) subjects, who were interested in participating in the study
- Appendix F; The informed consent form (written in Dutch) regarding participation in this study.

I would like to thank my supervisors Frans van der Helm, Annemarijn Steijlen, Kaspar Jansen and Edwin Goedhart for their support, feedback and guidance during this period. Also, I'd like to express my highest gratitude to the KNVB SMC for allowing me to use their technology, for all the support during my research and for the great time. I would especially like to thank Erik Wilmes, Jasper van der Zon and Bram Bastiaansen for their help, support and for their advices which were from the perspective of a human movement scientists. I'd also like to express my gratitude to the participants for volunteering, without them the research would not have been possible. Finally, I would like to thank Linda Plaude and my mother for the help with the design and construction of the Smart Sensor Shorts as this Master Thesis is based around this new measurement tool.

Suman Sukumar Vinasithamby
Beverwijk, 18th of June 2019

Table of contents

Scientific paper	9
I. INTRODUCTION	10
II. METHODS.....	11
A. Subjects	11
B. Instrumentation	11
C. Testing protocol	11
D. Data analysis	12
III. RESULTS	13
IV. DISCUSSION	16
ACKNOWLEDGMENT	19
References	19
Authors.....	20
A Construction of the Smart Sensor Shorts.....	21
A.1. Design phase	21
A.2. Construction phase.....	23
A.2.1. Parts list	23
A.2.2. Sewing	24
A.2.3. Soldering	25
A.2.4. Casting.....	27
A.3. Programming phase	28
A.4. Calibration IMUs	28
A.4.1. Calibration of the accelerometer.....	29
A.4.2. Calibration of the gyroscope.....	29
A.4.3. Calibration of the magnetometer	29
B Optimization of kinematic data	32
B.1. IMU to Segment calibration.....	33
B.2. β gain.....	34
C Concurrent validation internship report.....	37
C.1. Introduction.....	37
C.2. KNVB Sport Medisch Centrum	38
C.3. Methods.....	39
C.3.1. Subjects.....	39
C.3.2. Instrumentation	39
C.3.3. Testing protocol	41
C.3.4. Data analysis	42
C.4. Results.....	42
C.5. Discussion	43
C.6. Conclusion and recommendations	44

D	Test protocol (Dutch)	46
E	Information letter (Dutch)	49
F	Informed Consent (Dutch).....	51
	References.....	54

Scientific paper

Smart Sensor Shorts: Prevention of hamstring injuries in professional and recreational football athletes by analyzing and monitoring kinematic data

Suman S. Vinasithamby¹, Erik Wilmes², Annemarijn S.M. Steijlen³, Kaspar M.B. Jansen⁴, Edwin A. Goedhart⁵, Frans C.T. van der Helm⁶

Abstract- Multiple studies indicated that the degree of muscle strain is the most relevant parameter in understanding the injury mechanism behind a hamstring strain injury. To monitor this parameter a new system is developed; the Smart Sensor Shorts. The system contains five Inertial Measurement Units (IMUs) integrated in a sports tights. The purpose of this study was to develop a methodology to estimate the muscle strain and muscle elongation velocity of the biceps femoris (BF), semimembranosus (SM) and the semitendinosus (ST) muscle in professional and recreational football athletes with the use of IMUs during different football specific movements and during different intensities. When comparing different movements and intensities, the greatest peak muscle strain was found in the BF and the lowest peak muscle strain was found in the SM during the majority of the movements. The biomechanical load was different for each hamstring muscle and was different for the running based movements and other football specific movements. The BF experienced the greatest peak muscle strain ($12.12 \pm 0.88\%$) during a maximal intensity kick in the supporting leg, while the greatest peak muscle elongation velocity was observed in the ST ($3.97 \pm 0.47 \text{ s}^{-1}$) in the kicking leg during the maximal intensity kick. The greatest biomechanical loading was during a maximal intensity kick. Finally, it was observed that the moment of peak muscle strain was different from the time period of peak muscle elongation velocity for running based movements. It is concluded that IMUs together with the developed methodology could be used in the assessment of hamstring strain injuries in professional and recreational football by analyzing and monitoring muscle strain and muscle elongation velocity.

Index Terms- Injury prevention, Inertial Measurement Unit, biomechanics, football, muscle strain injury

I. INTRODUCTION

Muscle injuries constitute more than a third of all time-loss injuries in football and field hockey and cause more than a quarter of the total injury absence, with the hamstrings and adductors being the most frequently involved (Ekstrand et al., 2016). Despite diverse efforts on prevention of muscle injuries, there is an annual increase of hamstring injuries in professional football. An important reason for this type of injuries is the high muscle stress during explosive actions like sprinting, directional changes, jumping and kicking in modern game-play (Barnes et al., 2014).

However, the currently available monitoring systems are not able to measure the load of the musculoskeletal system around the hip for this particular objective. Optoelectronic Motion Analysis Systems are nowadays used in human motion analysis and biomechanical research to accurately estimate kinematic data (Giagazoglou et al., 2011; Inoue et al., 2014). However, they have some limitations; limited portability, require complex set-ups, are constrained to small test areas and to mainly laboratory settings. For this reason a new monitoring system is developed, the Smart Sensor Shorts. The system contains five Inertial Measurement Units (IMUs) integrated in a sports tights (i.e. shorts) and placed on different locations on the lower extremity.

An IMU consists out of three types of sensors; accelerometer, gyroscope and magnetometer which measures the acceleration, angular velocity and magnetic field, respectively in three different directions with respect to a body segment (Roetenberg et al., 2007; Roetenberg et al., 2013). With the use of sensor fusion algorithms (an algorithm that combines the three raw data sets of the individual sensors to estimate orientation) and a biomechanical model, joint kinematics could be estimated (Roetenberg et al., 2013).

IMUs have already been used to analyze sport-specific movements e.g. running (Reenalda et al., 2016), kicking (Blair et al., 2018). Besides, the concurrent validation of the Smart Sensor Shorts showed good agreement with an Optoelectronic Motion Analysis System (Appendix C). This indicates that IMUs could be used to accurately estimate human motion kinematics and to substitute Optoelectronic Motion Analysis Systems to perform sport-specific measurements on the playing field (outdoor). A combination of multiple IMUs attached to different body segments of interest (i.e. Smart Sensor Shorts) overcome the limitations of Optoelectronic Motion Analysis Systems by allowing measurements without the restriction of a measuring volume.

In the literature, it was found that the most important parameter to predict a hamstring strain injury is the hamstring muscle strain. A significant increase in peak value of the hamstring muscle strain during the terminal swing phase of running could result in a hamstring strain injury (Schache et al., 2012; Schache et al., 2010; Heiderscheidt et al., 2005; Chumanov et al., 2007; Chumanov et al., 2011). These studies indicated that the degree of muscle strain is most relevant parameter in understanding the injury mechanism behind a hamstring strain injury. This conclusion is consistent with

the results found in an animal based study (Lieber and Fridén, 1993); “whereby muscle damage after an eccentric contraction was found not simply to be a function of peak muscle force but rather was due to the magnitude of the strain experienced by the musculotendon unit during contraction” (Schache et al., 2012). However, it is not known if measurements of kinematic data of the lower extremity with the use of IMUs could be converted to an estimate of the muscle elongation of the individual hamstring muscles and eventually be used to compute the muscle strain and the muscle elongation velocity. The computed parameters could then be monitored regarding certain thresholds, where after the probability of the occurrence of a hamstring strain injury in professional and recreational football athletes could be quantified.

The objective of this study is to develop a methodology to estimate the muscle strain and muscle elongation velocity of the bicep femoris (BF), semimembranosus (SM) and semitendinosus (ST) muscles in professional and recreational football athletes with the use of IMUs.

II. METHODS

A. Subjects

Eight recreational athletes (7 men, 1 women, age of 23.6 ± 2.00 years; height of 178.8 ± 9.54 cm and mass of 72.9 ± 8.40 kg) provided written informed consent to participate in this research study approved by the Delft University of Technology Ethics Committee. All participants were regularly active in some type of sports (e.g. football, running).

B. Instrumentation

Participants wore the Smart Sensor Shorts, which is a Nike Pro Tights (Nike Inc., Beaverton, United States of America) integrated with five MPU-9250 IMUs (InvenSense Inc., San Jose, United States of America) and an Arduino Due (101.52×53.3 mm: 36 g), Prototyping Shield PCB, I²C Multiplexer board, MicroSD Breakout board plus MicroSD card 128 GB UHS class 3, LiPo AccuPack battery and PowerBoost 500 Basic board zipped into a waist pack (290 x 100 x 60 mm) which is attached to the rear end of the tights (Fig. 1). Each IMU (dimensions: 18 x 17 mm) consists out of a 3D accelerometer (range: $\pm 32g$, noise: $300 \mu g/\sqrt{Hz}$), a 3D gyroscope (range: $\pm 2000^\circ/s$, noise: $0.01 \text{ deg./sec}/\sqrt{Hz}$) and a 3D magnetometer (range: $\pm 4800\mu T$). The Smart Sensor Shorts has a mean sample rate of 165 ± 17.5 Hz. However, the Δt (i.e. equal to $1/\text{sample frequency}$) is estimated at each sample point. The IMUs are sewed on the tights, where after the IMUs are casted with silicone rubber for a more stable fixation and for protection against external factors (e.g. sweat, rain, impact). The IMUs are connected to the hardware modules by coated copper wires. After soldering, these wires are sewed on to the tights in a wave pattern. The wave pattern is able to stretch along with the fabric, so that fracture of the wires due to stretching of the skin (caused by movements performed and/ or muscle contraction) and eventually due to stretching of the fabric is prevented (Appendix A).

Sensor to segment calibration is performed in two steps (i.e. static and dynamic) and is based on the study performed by

Luinge et al., 2007. The orthogonal local coordinate system of the each IMU is firstly rotated such that the y- axis is aligned with the gravity vector. This is done by letting the subject standstill for 10 sec. (static). Subsequently the subject is asked to perform three calibration movements (dynamic) (Appendix B).

- 1) The first movement is performed with one of the legs and is described as; from the neutral rest position (i.e. upright stance), to a position where the knee (0 deg.) and hip (± 30 deg.) are extended (the position needs to be held for 2 sec.), to a position where the knee (± 30 deg.) and hip (± 45 deg.) are flexed and eventually back to the neutral rest position. In the neutral rest position the knee and hip flexion/ extension joint angle are equal to 0 deg.
- 2) The second movement is the same as the first movement but with the other leg.
- 3) The third and final movement is performed with the trunk and is described as; from the neutral rest position, to a position where the trunk is flexed (± 45 deg.) and back to the neutral rest position.

It is important that all three movements are performed in the sagittal plane.

By letting the subject execute these movements, the sagittal plane of the left leg, right leg and pelvis is estimated, where after the rotated local coordinate systems of the IMUs are rotated such that the z- axis is perpendicular to the sagittal plane of the corresponding side (Fig. 2). As the placement of the sensors on each side (left, right and center) of the Smart Sensor Shorts is different, three movements are performed such that three different sagittal planes could be estimated. No magnetic disturbances were reported in the testing environment (Appendix A).

C. Testing protocol

All subjects wore either (outdoor) football shoes with studs or running shoes. Subjects performed multiple warm- up sprints on their own preference followed by the sensor to segment calibration. Where after, the subjects were instructed to perform seven different football specific movements on two intensities i.e. “moderate” and “maximal” for one repetition (Table 1.). Pawns were set up at three specific locations (i.e. 0m, 5m and 10m) inside the measuring volume (Fig. 1).

Table 1. The seven different football specific movements based on Stevens et al. (2014) described for two intensities, moderate and maximal. Each movement is performed for one repetition on two intensities, where after the next movement is performed.

Intensity: moderate	Intensity: maximal
10m jog	10m sprint
10m jog- rapid stop	10m sprint- rapid stop
10m jog- change of direction 180 deg.	10m sprint- change of direction 180 deg.
5m jog- change of direction 45 deg.	5m sprint- change of direction 45 deg.
5m jog- forward- backward	5m sprint- forward- backward
pass	kick
jump from standstill	jump with run- up



Fig. 1
The experimental test set-up used in this research study. The subject wearing the Smart Sensor Shorts (top) and the measuring volume (bottom). The locations of the five IMUs on the Smart Sensor Shorts are indicated with the orange circles (top left and top center).

D. Data analysis

Data analysis was performed in Matlab (Mathworks, Natick, United States of America). Raw accelerometer and gyroscope data were filtered using a low-pass 4th order Butterworth filter (cut-off frequency: 12 Hz). Type of filter and cut-off frequency were chosen based on findings in the current literature (Blair et al., 2018; Winter, 2009). Orientation estimation regarding the IMUs in the Smart Sensor Shorts were performed with a sensor fusion algorithm (based on the Madgwick Filter). Eight kinematic parameters were chosen as important to hamstring strain injuries in football and to eventually estimate the muscle strain and muscle elongation velocity. These parameters are the left and right sagittal plane knee and hip joint angles and the left and right sagittal plane knee and hip joint angular velocities. After the orientation of each IMU is estimated, joint angles could be calculated by determining the orientation of the most distal IMU relative to the proximal one using a Z-Y-X Cardan sequence. The sagittal plane knee and hip joint angles were calculated as anatomical angles, with the knee measured as the angle between the thigh and the shank and the hip measured as the angle between the pelvis and the thigh.

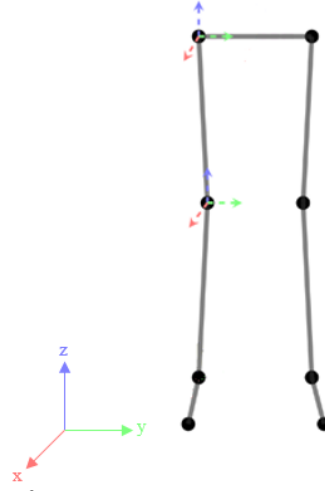


Fig. 2
A skeleton with the orthogonal local coordinate systems of the hip and knee joint for the right leg, analogous for left leg (Zimmermann et al., 2018).

The muscle elongation of the individual hamstring muscles was estimated as following:

$$\Delta l = (r_k \cdot \Delta\theta_k) + (r_h \cdot \Delta\theta_h) \quad (1)$$

Where r_k is the moment arm of a hamstring muscle relative to the knee joint, $\Delta\theta_k$ the change in knee joint angle relative to the knee joint angle in the neutral position (upright stance), r_h the moment arm of the individual hamstring muscle relative to the hip joint and $\Delta\theta_h$ the change in hip joint angle relative to the hip joint angle in the neutral position. In the neutral position the knee joint angle and hip joint angle are equal to 0 deg. The moment arms of the biceps femoris, semimembranosus and semitendinosus relative to the hip joint and the moment arm of the semitendinosus relative to the knee joint were based on an experimental study (Thelen et al., 2005). The moment arms of the biceps femoris and the semimembranosus relative to the knee joint were based on a cadaveric study (Herzog and Read, 1993). The moment arms change with increasing hip flexion and knee flexion angle. The model predictions of the moment arms based on the experimental study were eventually compared and validated with the experimental data of in vivo measurement studies (Arnold et al., 2000 and Buford et al., 1997). The muscle strain of the hamstring muscles was estimated by normalizing the muscle elongation (Equation 1) with the muscle-tendon length in the neutral rest position (l_{ref}) (Table 2). Note that the muscle-tendon length in the neutral rest position is not equal to the optimal length of the hamstring muscles.

The elongation velocity of the hamstring muscles was estimated as the first time derivative of Equation 1:

$$v_e = (r_k \cdot \omega_k) + (r_h \cdot \omega_h) \quad (2)$$

Where ω_k is the angular velocity of the knee joint and ω_h the angular velocity of the hip joint. Eventually the muscle elongation velocity (Equation 2) is normalized to the muscle-tendon length in the neutral rest position (l_{ref}). A specific muscle elongation velocity induces a greater biomechanical loading on shorter muscle-tendon units compared with muscles with a greater muscle-tendon length. By normalizing the muscle

elongation velocity, the influence of (optimal) muscle- tendon length on the biomechanical loading of the muscle due to amount of muscle elongation is included. Due to technical problems (hardware failure) the motion data of some movements of four subjects could not be collected and thus not analyzed.

Table 2. Presentation of the three musculoskeletal model parameters, which serve as input for the estimation of the muscle strain and muscle elongation velocity of the individual hamstring muscles; cadaveric length of the hamstring muscle-tendon (lref) and (cadaveric) moment arm of the hamstring muscles around the hip and knee joint. The muscle- tendon lengths are expressed for the neutral position, i.e. upright stance, this means a neutral hip angle (0 deg.) and a neutral knee angle (0 deg.). Moment arms changing with increasing hip flexion angle are presented for neutral hip angle (0 deg.) and flexed hip angle (45 to 50 deg.). Subsequently, moment arms changing with increasing knee flexion angle are presented for neutral knee angle (0 deg.) and flexed knee angle (30 to 35 deg.).

Hamstring muscle	Muscle- tendon length	Moment arm hip	Moment arm knee
Biceps femoris	43.8 cm	neutral; 4.7 cm flexed; 5.8 to 5.9 cm	neutral; 1.5 cm flexed; 2.8 to 3.2 cm
Semimembranosus	43.9 cm	neutral; 3.6 cm flexed; 4.8 to 4.9 cm	neutral; 2.8 cm flexed; 4.2 to 4.7 cm
Semitendinosus	44.3 cm	neutral; 4.8 cm flexed; 6.6 cm	neutral; 3.6 cm flexed; 4.6 to 4.7 cm

III. RESULTS

Multiple parameters were chosen as important in; 1) distinguishing the difference between the “moderate” intensity and the “maximal” intensity and 2) assessing the validity of the joint angles and joint angular velocities estimated by the Smart Sensor Shorts during the different movements and intensities compared with results found in the literature. The mean (running) speeds for the running based football specific movements are estimated by integrating the accelerometer data obtained from the IMU on the pelvis and are defined in Table 3. The peak knee angular velocity of the kicking leg and the flexion/ extension angle of the hip and the knee of the left and right leg are estimated with the use of the Smart Sensor Shorts.

The peak muscle strain and peak muscle elongation velocity of each of the individual hamstring muscles were greater for the maximal intensity compared with the moderate intensity (Table 4, Table 5, Fig. 2). The peak values of the muscle strain were the greatest in the biceps femoris then in the semitendinosus and the lowest in the semimembranosus during the majority of the movements. Exceptions are; 1) during a maximal kick; the peak muscle strain is the greatest in the semitendinosus of the kicking leg and 2) for a moderate jump; the peak muscle strain is the lowest in the semitendinosus. The peak values of the muscle elongation velocity were the greatest in the semitendinosus and the lowest in the semimembranosus during all movements, except for the moderate intensity jump. During the moderate intensity jump, the greatest peak muscle elongation velocity was in the biceps femoris.

Table 3. Kinematic means (SD) across eight subjects and one repetition of the most important parameters to distinguish the two different intensities (column parameter) of the football specific movements and the means of the maximum knee flexion angle and maximum hip flexion angle for the left (L) and right (R) leg. For the kicking movements, the subjects are divided into two groups; subject who kicked with the left leg (L) and subject who kicked with the right leg (R).

Movement	Parameter		Maximum knee flexion angle (deg.)	Maximum hip flexion angle (deg.)
Sprint <i>Moderate</i>	Running speed (m/s)	2.90 (0.59)	L: 99.55 (13.03) R: 104.01 (12.91)	L: 51.34 (11.96) R: 54.43 (11.94)
	Running speed (m/s)	4.92 (0.82)	L: 117.45 (12.58) R: 120.24 (8.70)	L: 70.79 (10.68) R: 73.31 (10.42)
Rapid stop <i>Moderate</i>	Running speed (m/s)	1.92 (0.40)	L: 102.13 (10.21) R: 104.34 (8.43)	L: 57.20 (9.36) R: 55.11 9.99
	Running speed (m/s)	2.22 (0.24)	L: 109.66 (10.23) R: 111.34 (9.75)	L: 69.25 (11.77) R: 70.49 (10.03)
Change of direction 180 deg. <i>Moderate</i>	Running speed* (m/s)	2.16 (0.21)	L: 102.00 (7.68) R: 104.72 (14.36)	L: 60.70 (11.78) R: 59.55 (12.58)
	Running speed* (m/s)	2.49 (0.43)	L: 114.15 (7.93) R: 109.66 (9.47)	L: 72.44 (13.19) R: 71.80 (12.00)
Change of direction 45 deg. <i>Moderate</i>	Running speed (m/s)	3.10 (0.60)	L: 103.54 (15.99) R: 103.57 (16.92)	L: 50.14 (9.82) R: 54.53 (8.77)
	Running speed (m/s)	4.70 (0.62)	L: 106.11 (15.81) R: 112.73 (10.94)	L: 71.99 (9.02) R: 76.54 (6.37)
Forward- backward <i>Moderate</i>	Running speed* (m/s)	2.05 (0.27)	L: 99.76 (9.33) R: 95.60 (10.95)	L: 55.90 (13.15) R: 58.34 (12.36)
	Running speed* (m/s)	2.37 (0.34)	L: 100.91 (6.36) R: 105.86 (6.64)	L: 69.13 (9.09) R: 72.87 (8.55)
Kick <i>Moderate</i>	Peak angular velocity knee kicking leg (deg./s)	L: 823.99 (5.55) R: 1057.13 (350.78)	L: 89.90 (14.73) R: 92.48 (14.26)	L: 58.24 (10.13) R: 47.16 (8.46)
	Peak angular velocity knee kicking leg (deg./s)	L: 1665.37 (313.96) R: 1653.61 (215.10)	L: 97.49 (12.33) R: 98.63 (10.21)	L: 70.74 (10.66) R: 65.53 (7.96)
Jump <i>Moderate</i>	Speed z- direction (m/s)	2.55 (0.22)	L: 79.46 (10.16) R: 75.61 (13.84)	L: 68.43 (17.44) R: 69.25 (17.67)
	Speed z- direction (m/s)	2.79 (0.31)	L: 88.75 (10.63) R: 85.66 (13.27)	L: 59.60 (10.62) R: 63.51 (7.77)

*the running speed is estimated based on the strides prior to change of direction

Table 4. Means (SD) across eight subjects and one repetition of the peak muscle strain (%) of biceps femoris, semimembranosus and semitendinosus muscles during a 10m sprinting, 10m rapid stop, 10m change of direction 180 deg, for the dominant (D) and supporting (S) leg, 5m change of direction 45 deg., 5m forward-backward, kicking, for the kicking (K) and supporting leg, and jumping movement on a moderate and maximal intensity.

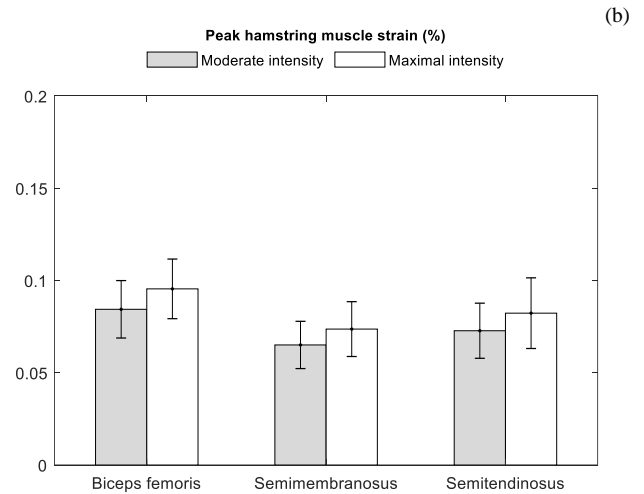
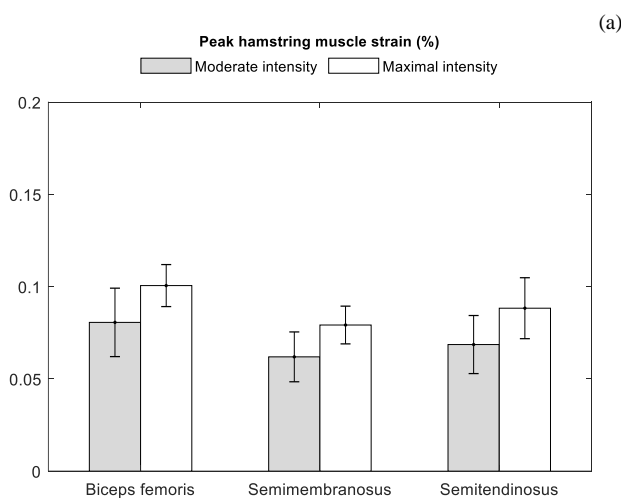
Movement	Intensity	Peak muscle strain (%)			
		BF	SM	ST	
Sprint	Moderate	8.06 (1.85)	6.19 (1.35)	6.86 (1.57)	
	Maximal	10.06 (1.14)	7.92 (1.02)	8.83 (1.65)	
Rapid stop	Moderate	8.36 (2.27)	6.53 (2.10)	7.44 (2.69)	
	Maximal	9.55 (1.62)	7.37 (1.49)	8.23 (1.92)	
Change of direction 180 deg.	Moderate	D:	8.36 (2.27)	6.53 (2.10)	7.44 (2.69)
		S:	8.63 (2.06)	6.59 (1.84)	7.20 (2.44)
	Maximal	D:	9.88 (1.54)	7.72 (1.49)	8.63 (2.11)
		S:	9.91 (1.56)	7.96 (1.43)	9.22 (1.83)
Change of direction 45 deg.	Moderate	8.20 (1.68)	6.47 (1.44)	7.39 (1.79)	
	Maximal	10.52 (1.07)	8.43 (1.46)	9.74 (2.29)	
Forward-backward	Moderate	8.44 (1.70)	6.57 (1.56)	7.42 (1.98)	
	Maximal	11.52 (5.55)	9.88 (6.89)	9.10 (1.68)	
Kick	Moderate	K:	8.49 (1.51)	6.93 (1.56)	7.86 (2.51)
		S:	10.18 (1.76)	8.30 (1.37)	9.62 (1.61)
	Maximal	K:	11.12 (1.29)	9.59 (1.47)	11.42 (2.06)
		S:	12.12 (0.88)	9.83 (0.81)	11.45 (1.21)
Jump	Moderate	7.60 (1.60)	5.62 (1.43)	5.30 (1.98)	
	Maximal	9.42 (1.74)	7.27 (1.65)	7.83 (2.42)	

For the change of direction 180 deg. movement, there is no significant difference in peak muscle strain and peak muscle elongation velocity between the dominant (i.e. cutting) leg and the supporting leg (Table 4, Table 5, Fig.2). The movement could be executed in two ways, cutting to left or right, in contrast to the change of direction 45 deg. which could only be executed in one way due to the test set-up.

Table 5. Means (SD) across eight subjects and one repetition of the peak elongation velocity (m/s) of biceps femoris, semimembranosus and semitendinosus muscles during a 10m sprinting, 10m rapid stop, 10m change of direction 180 deg, for the dominant (D) and supporting (S) leg, 5m change of direction 45 deg., 5m forward-backward, kicking, for the kicking (K) and supporting leg, and jumping movement on a moderate and maximal intensity.

Movement	Intensity	Peak normalized muscle elongation velocity (s ⁻¹)			
		BF	SM	ST	
Sprint	Moderate	1.02 (0.19)	0.87 (0.15)	1.25 (0.20)	
	Maximal	1.82 (0.19)	1.46 (0.14)	2.07 (0.25)	
Rapid stop	Moderate	1.15 (0.16)	0.98 (0.13)	1.41 (0.17)	
	Maximal	1.78 (0.21)	1.49 (0.16)	2.16 (0.26)	
Change of direction 180 deg.	Moderate	D:	1.19 (0.22)	1.01 (0.13)	1.45 (0.15)
		S:	1.21 (0.24)	1.03 (0.20)	1.50 (0.26)
	Maximal	D:	1.87 (0.20)	1.57 (0.12)	2.22 (0.21)
		S:	1.75 (0.22)	1.47 (0.15)	2.09 (0.21)
Change of direction 45 deg.	Moderate	1.05 (0.15)	0.89 (0.11)	1.29 (0.14)	
	Maximal	1.76 (0.21)	1.47 (0.19)	2.10 (0.27)	
Forward-backward	Moderate	1.12 (0.24)	0.99 (0.18)	1.45 (0.26)	
	Maximal	1.70 (0.16)	1.45 (0.11)	2.09 (0.18)	
Kick	Moderate	K:	1.99 (0.56)	1.86 (0.49)	2.79 (0.77)
		S:	1.12 (0.25)	0.98 (0.19)	1.45 (0.26)
	Maximal	K:	2.65 (0.31)	2.51 (0.28)	3.97 (0.47)
		S:	1.47 (0.23)	1.29 (0.18)	1.89 (0.27)
Jump	Moderate	0.56 (0.15)	0.46 (0.12)	0.49 (0.13)	
	Maximal	0.96 (0.39)	0.86 (0.33)	1.23 (0.50)	

The maximal intensity kick resulted in the greatest biomechanical loading on the hamstring muscles among the different movements and intensities, as the peak muscle strains were the greatest in the supporting leg, while the peak muscle elongation velocities were the greatest in the kicking leg (Table 4, Table 5, Fig. 3); BF ($12.12 \pm 0.88\%$ and $2.65 \pm 0.31\text{ s}^{-1}$), SM ($9.83 \pm 0.81\%$ and $2.51 \pm 0.28\text{ s}^{-1}$) and ST ($11.45 \pm 1.21\%$ and $3.97 \pm 0.47\text{ s}^{-1}$). Running based movements resulted in the second greatest peak muscle strains and muscle elongation velocities, with the maximal intensity 5m forward- backward movement resulting in the greatest peak muscle strains and the maximal intensity 10m change of direction 180 deg. movement resulting in the greatest peak muscle elongation velocities (Table 4).



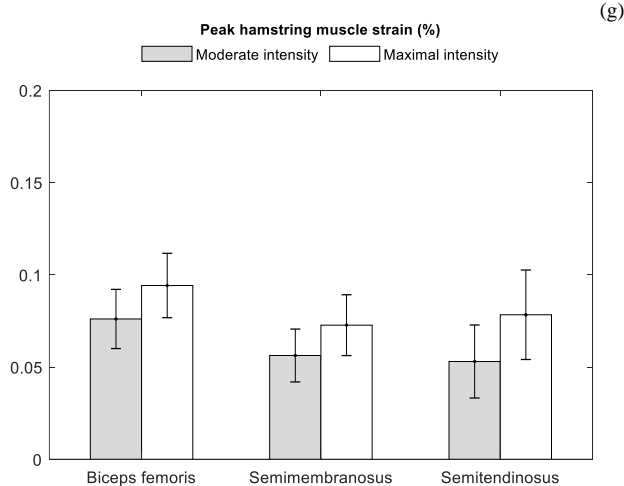
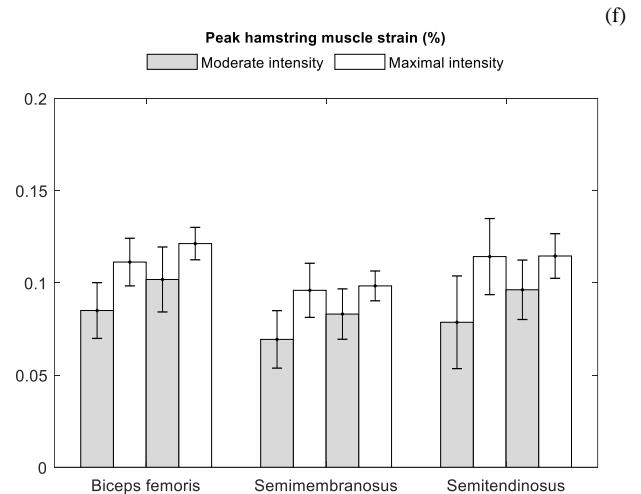
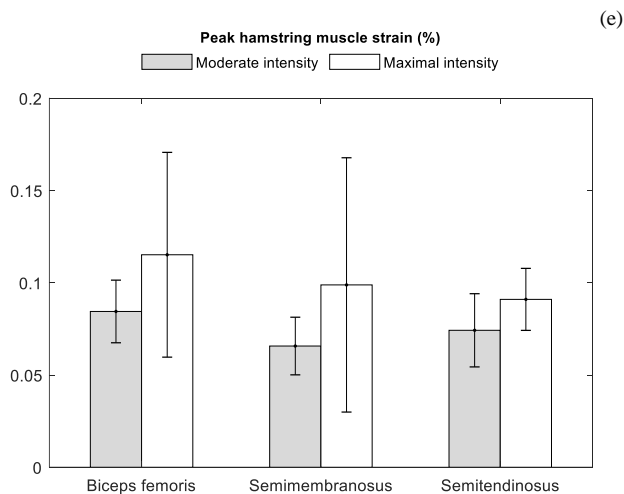
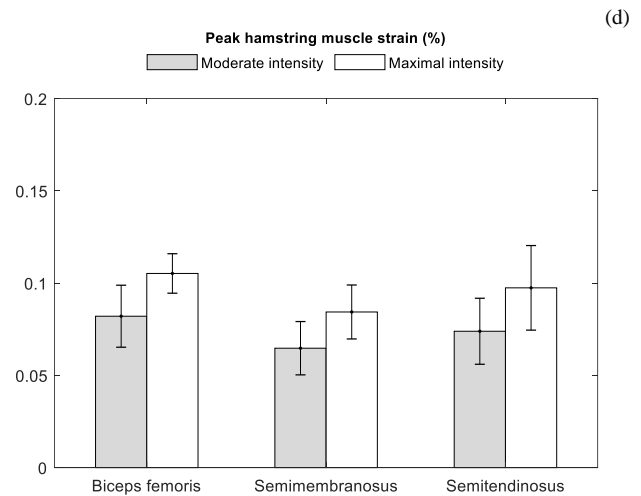
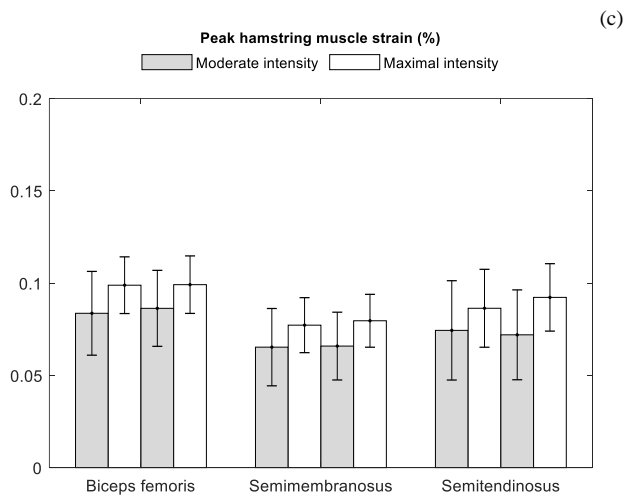


Fig. 3. Comparison of the peak muscle strain of the biceps femoris, semimembranosus and semitendinosus muscles during a 10m sprinting (a), rapid stop (b), 10m change of direction 180 deg. (c), 5m change of direction 45 deg. (d), 5m forward- backward (e), kicking (f) and jumping (g) movement on a moderate and maximal intensity. For the 10m change of direction 180 deg. and kicking movement, bars for both the dominant/ kicking leg and supporting leg are presented, respectively.

The moment that peak muscle strain is reached in the hamstring muscles is different from the time period of peak muscle elongation velocity during running based (continuous) movements (Fig. 4). For the kicking movement, the peak muscle strain is found in the time period that peak muscle elongation velocity is reached. However, during a jumping movement, the peak muscle strain is found during the movement before the actual jump; the run up, which is a continuous movement. However, it could also occur that peak muscle strain is observed in the time period that peak muscle elongation velocity is reached as can be seen during a change of direction 45 deg. movement in Fig. 4.

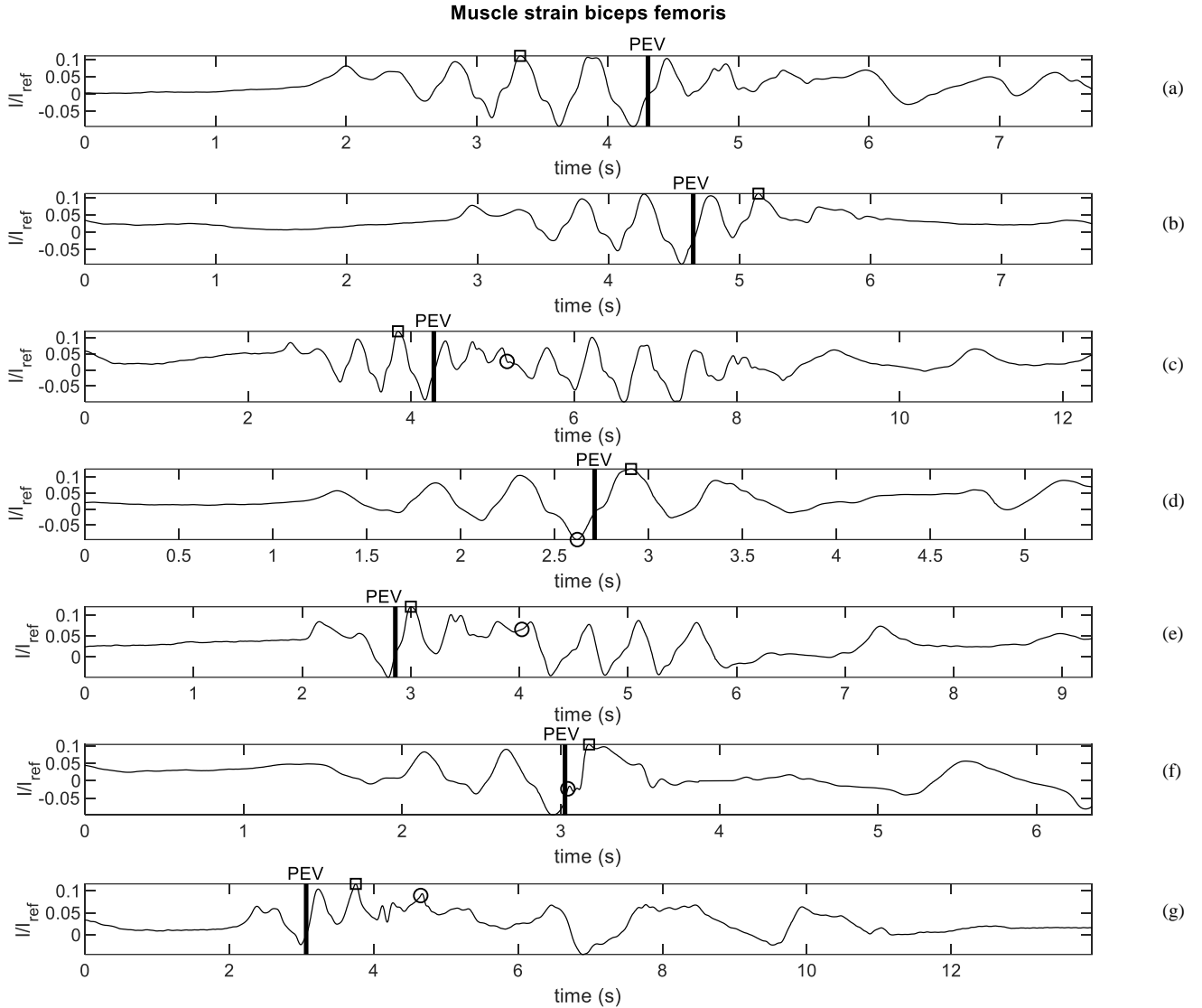


Fig. 4. The muscle elongation of the biceps femoris muscle of the dominant (preferred) leg estimated with the use of the Smart Sensor Shorts during a 10m sprinting (a), 10m rapid stop (b), 10m change of direction 180 deg. (c), 5m change of direction 45 deg. (d), 5m forward- backward (e), kicking (f) and jumping (g) movement on maximal intensity of one typical subject (PEV = moment that peak elongation velocity is reached). The peak muscle strain and the moment of execution of the actual movement (c, d, e, f and g) are indicated by \square and \circ , respectively.

IV. DISCUSSION

The objective of this study was to develop a methodology to estimate the muscle strain and muscle elongation velocity of the bicep femoris, semimembranosus and semitendinosus muscles with the use of IMUs. It is concluded that IMUs could be used to estimate these parameters based on the following results.

- 1) When comparing the individual hamstring muscles, the greatest peak muscle strain was found in the biceps femoris and the lowest peak muscle strain was found in the semimembranosus during the majority of the movements (Table 4). Exceptions are the maximal intensity kick; greatest peak muscle strain in the semitendinosus and lowest peak muscle strain in the semimembranosus and the moderate intensity jump; greatest peak muscle strain in the biceps femoris and lowest peak muscle strain in the semitendinosus. The greatest peak muscle elongation velocity was found in the

semitendinosus and the lowest peak muscle elongation velocity was found in the semimembranosus for all movements aside from the moderate jump, where the greatest muscle elongation velocity is found in the biceps femoris (Table 5).

- 2) When comparing the different movements and intensities, the biceps femoris had the greatest peak muscle strain (12.12% increase in muscle length) for a maximal intensity kick in the supporting leg and the greatest muscle elongation velocity was observed in the semitendinosus (3.97 s^{-1}) for a maximal intensity kick in the kicking leg.
- 3) During a kicking movement, the peak muscle strain is greater for the supporting leg than for the kicking leg. However, the greatest peak muscle elongation velocity is observed in the kicking leg, namely in the semitendinosus.

- 4) Between the different football specific movements, the peak muscle strain and peak muscle elongation velocity are the greatest for the maximal intensity kick in all three hamstring muscles, which indicates that the hamstring muscles experienced the greatest biomechanical loading during a maximal intensity kick (Table 4, Table 5).
- 5) The moment that peak muscle strain is reached is different from the time period that peak elongation velocity is observed for “continuous movements” (i.e. running based movements) (Fig. 4).

When measuring sagittal knee and hip joint angles and joint angular velocities, the findings in this study (Table 3) are comparable with the studies found in the current literature regarding joint kinematics during running based movements (Riley et al., 2008; running speed: 3.84 ± 0.64 m/s; min. knee flexion angle: 110.1 ± 18.4 deg.; Reenalda et al., 2016; running speed: 4.08 ± 0.61 m/s; min. knee flexion angle: 94.01 ± 1.19 deg.; max. hip flexion angle: 51.78 ± 1.58 deg.), kicking movements (Blaire et al., 2018; angular velocity knee kicking leg: 1309 deg./s; min. knee flexion angle: 104 deg.; max. hip flexion angle: 47.9 deg.; Kellis et al., 2007; angular velocity knee kicking leg: 1206 ± 218 to 1874 ± 155 deg./s) and jumping movements (Yu et al., 2006; min. knee flexion angle: 77.36 ± 10.59 deg.; max. hip flexion angle: 55.93 ± 14.55 deg.; Chappell et al., 2008; min. knee flexion angle: 81.00 ± 9.10 deg.; max. hip flexion angle: 82.00 ± 10.40 deg.). The difference in maximum hip flexion angle for jumping and kicking movements could be explained by the execution of the movement. Yu et al. (2006) and Blaire et al. (2018) used a stop- jump task and a instep kick, respectively. However, in this study the jump and kick could be performed to the subject's preference, which is for instance seen during the kicking movement as some subjects kicked with the inside of their foot and some used a instep kick technique. Besides, Blaire et al. (2018), estimated the joint kinematics of kicking at ball contact, while this study also includes the kinematics after ball contact. The concurrent validity study between the Smart Sensor Shorts and an Optoelectronic Motion Analysis System found that the Smart Sensor Shorts estimated sagittal knee and hip joint angles with a 2.79 to 7.37 deg. RMS orientation error compared to the golden standard (Appendix C). As the majority of the studies used an Optoelectronic Motion Analysis System to estimate the joint kinematics, the difference in kinematic values was partly caused by the RMS orientation error.

The peak muscle strain of the individual hamstring muscles during (over ground) sprinting found in the current study (Table 4) were consistent with that reported in the current literature (Yu et al., 2008; Thelen et al., 2005; running speed: 8.75 m/s; peak muscle strain; BF: 1.098, SM: 1.075 and ST: 1.082; Chumanov et al., 2007; running speed: 8.64 m/s; peak muscle strain; BF: 11.69%, SM: 9.70% and ST: 9.68%; Chumanov et al., 2011; running speed: 7.55 m/s, peak muscle strain; BF: 1.13, SM: 1.11 and ST: 1.10; Wan et al., 2017; running speed: 7.97 m/s, peak muscle strain; BF: 7.8%, SM: 7.0% and ST: 7.8%; Heiderscheit et al., 2005; running speed: 4.47 m/s, peak muscle strain; BF: 1.121, SM: 1.096 and ST: 1.102; Schache et al., 2009; running speed: 7.44 m/s; peak muscle strain right and left leg; BF: 12.90%, 10.63%, SM: 11.60%, 9.70% and ST: 11.10% and 8.69%, respectively; Schache et al., 2012;

running speed: 8.95 m/s; peak muscle strain; BF: 11.98%, SM: 9.84% and ST: 8.73%). The differences between the results of this study and the results found in the current literature are caused by the difference in intensity, as the running speeds observed in the literature are greater compared with the running speeds obtained during the running based movements (Table 3). The results of this study also indicates that the greater the running speed, the greater the peak muscle strain and the greater the peak muscle elongation velocity, which is consistent with the results found in the literature.

The peak muscle elongation velocity of the individual hamstring muscles during (over ground) sprinting found in the current study; running speeds: 2.90 m/s and 4.90 m/s; peak muscle elongation velocity; BF: 1.02 s^{-1} (0.45 m/s) and 1.82 s^{-1} (0.80 m/s); SM: 0.87 s^{-1} (0.39 m/s) and 1.46 s^{-1} (0.65 m/s); ST: 1.25 s^{-1} (0.55 m/s) and 2.07 s^{-1} (0.91 m/s), respectively were in some cases consistent with that reported in the current literature (Yu et al., 2008; Schache et al., 2010; running speeds: 1.97 m/s and 7.44 m/s; peak muscle elongation velocity: 0.30 m/s and 0.50 m/s, respectively; Schache et al., 2012; running speed: 8.95 m/s; peak muscle elongation velocity; BF: 0.96 m/s, SM: 0.84 m/s and ST 1.04 m/s; Thelen et al., 2005; running speed: 8.75 m/s; peak muscle elongation velocity; BF: 1.77 m/s, SM: 1.71 m/s and ST: 1.93 m/s). It could be observed, that the results found in the current literature differ greatly among studies in terms of reported muscle elongation velocities. For this reason, it is difficult to compare the results of this study with that reported the current literature.

In the current literature there is one study which estimated the hamstring kinematics during a kicking movement. For a maximal instep soccer kick, the peak muscle strain and peak muscle elongation velocity found in the current literature for the kicking leg are; BF: 165.28%, 1.53 m/s, SM: 220.75%, 2.69 m/s and ST: 90.95% and 3.20 m/s, respectively (Sinclair, 2016). However, Schache et al. and Heiderscheit et al. identified the period of a hamstring strain injury at an estimated peak muscle strain of the biceps femoris of 12% (Heiderscheit et al., 2005) and 12.9% (Schache et al., 2009). This would mean that the subjects would experience a hamstring strain injury by performing a kicking movement as described by Sinclair (2016). Besides, the muscle-tendon lengths used in the study differ greatly from the lengths found in the current literature, which are scientifically evidenced with cadaver studies and which are used in this study (Table 2). The reported kinematics and the used muscle- tendon lengths falsify the findings of Sinclair (2016). However, the results of this study are consistent with observations from DeProft et al. (1988), which stated that during a soccer kick an activation (70 % of maximum voluntary contraction) is seen in the biceps femoris and semitendinosus in the kicking leg, as the peak muscle strain and peak muscle elongation velocity are the greatest in the semitendinosus and biceps femoris in the kicking leg.

In the current literature there are no studies found which estimated the hamstring muscle kinematics for a change of direction 45 deg., change of direction 180 deg., forward- backward and/ or jumping movement.

All studies found in the current literature used an Optoelectronic Motion Analysis System in combination with a musculoskeletal model to estimate the hamstring kinematics.

The results found in this study support the findings that the biceps femoris is the most commonly strained hamstring muscle (Opar et al., 2012; Woods et al., 2004) as the found peak muscle strains are the greatest in the biceps femoris during the majority of the football specific movements (Table 4). Subsequently, an injury study performed by the UEFA Elite Club reported that 70% of all hamstring injuries occurred during high speed running or sprinting (Ekstrand et al., 2016) in which the amount of accelerations and decelerations is increased. In this study, it was found that the greatest peak muscle strain occurred during a kicking movement followed by two running based movements (i.e. 5m forward backward movement and 10m sprinting movement, respectively). The running speeds in this study (Table 3) are relatively low compared with the running speeds observed in the current literature. This could explain the fact that the greatest peak muscle strain was found during a maximal intensity kick instead of a maximal intensity sprint, which is concluded to have the highest probability on the occurrence of a hamstring strain injury in professional football according to the UEFA Elite Club (Ekstrand et al., 2016). The greater peak muscle strain found during the maximal intensity 5m forward- backward movement compared with a maximal intensity 10m sprint is most likely caused due to the fact that the subject is forced to accelerate and decelerate in a short time period due to the relatively short distance (Ekstrand et al., 2016).

As for the maximal intensity kick, it was found that the supporting leg experienced a greater peak muscle strain compared with the kicking leg, while the peak muscle elongation velocity was greater for the kicking leg (Table 4, Table 5). During kicking, when the ball is located at a specific position, the subject needs to place his supporting leg next to the ball while his trunk stays in the same position. This step results in a flexed knee and hip and eventually in an great elongation of the hamstring muscles (Equation 1) before the kicking movement itself. The biomechanics of the maximal intensity kick depends on the technique used. The majority of the subjects kicked with the inside of their foot instead of with the upper surface of the foot (instep soccer kick). During a instep soccer kick, the extension of the hip is greater compared with a kick with the inside of the foot. A greater hip extension angle results in a greater hamstring muscle elongation and thus a greater hamstring muscle strain. The instep soccer kick results in a more powerful kick, which should burden the hamstring muscles more.

The time period that peak muscle elongation velocity is reached is different from the moment that peak muscle strain is observed during running based (continuous) movements (Fig. 4). The observation is consistent with results found in the current literature, as in multiple studies the time period of peak muscle elongation velocity and the moment of peak muscle strain are not directly related for running (Yu et al., 2008; Thelen et al., 2005; Schache et al., 2012). As it is already scientifically evidenced that hamstring muscle damage after an eccentric contraction was a function of the peak muscle strain experienced by the muscle-

tendon unit during contraction (Schache et al., 2012), the results in this study indicate that a hamstring strain injury could be a function of both the magnitude of the (peak) muscle strain and the magnitude of the (peak) muscle elongation velocity. During a kicking movement for instance, the peak muscle strains were the greatest in the supporting leg, while it is assumed that the kicking leg experienced a greater biomechanical loading due to greater muscle elongation velocities.

This study was associated with several limitations and assumptions.

- 1) The subjects only performed a single repetition per movement and per intensity. It is acknowledged that it would have been ideal to have analyzed multiple trials for each subject. However, to avoid the potential confounding effect of fatigue, the study was therefore limited to a single repetition per movement and per intensity for each subject.
- 2) The Smart Sensor Shorts has a relatively low sample frequency for analyzing football specific movements compared with sample frequencies used in the current literature (250 to 500 Hz). This is caused by limitations regarding the Arduino Due. To optimize the accuracy (concurrent validation) of the Smart Sensor Shorts relative to an Optoelectronic Motion Analysis System a higher sample frequency is needed.
- 3) The filter parameter(s) used for the sensor fusion algorithm are assumed to be a certain constant value (Appendix B). However, to optimize the accuracy of the estimation of the sagittal knee and hip joint angles a optimization study is needed regarding the filter parameter(s).
- 4) The muscle- tendon lengths and the moment arms of the bicep femoris, semimembranosus and semitendinosus relative to the knee and hip joint are derived from the current literature and are assumed to be equal for all subjects (Table 2). To obtain a more accurate result, the muscle- tendon lengths and moment arms need to be scaled to the subject.
- 5) The distance of the sprint was too short to achieve reasonable maximal sprint running speeds (7.55 to 8.75 m/s) as found in the current literature. To eventually compare and validate the results of the developed methodology with the results found in the current literature, the distance of the sprint needs to be increased.
- 6) The kicking and jumping movements were not strictly prescribed regarding execution of the movement. Studies found in the current literature which use the movements described the way to execute these movements (e.g. instep soccer kick, drop jump etc.). By letting the subject perform the movement at their own preference comparison and validation of the hamstring kinematics with the current literature is difficult.

This study found different biomechanical loads of the individual hamstring muscles during the different football specific movements; the greatest peak muscle strain was found during a maximal intensity kick in the biceps femoris of the supporting leg. However, the semitendinosus displayed the greatest peak muscle

elongation velocity in the kicking leg during a maximal intensity kick. The peak muscle strain and peak muscle elongation velocity were the greatest during the maximal intensity kick in the three individual hamstring muscles followed by two running based movements. It is concluded that kicking and running based movements have a high probability to the occurrence of a hamstring strain injury. Therefore, it is recommended that future work should be focused on kicking and running based movements. For the kicking movement, the main focus has to be on the difference between the biomechanical loading on the hamstring muscles of the kicking and supporting leg during an instep soccer kick and a kick with the inside of the foot. As for running based movements, the main focus has to be on the intensity. It is recommended to use distances, where running speeds as reported by studies found in the current literature could be achieved. Also, running based movements where rapid accelerations and decelerations need to be achieved are recommended to be used. Besides, it is recommended to develop a testing protocol in which the technique of movements such as kicking and jumping is prescribed to the subjects. Results could then easily be compared and validated with the current literature and there will not be any differences in results due to different techniques used. Subsequently, future research should be focused on the influences of a combination of (peak) muscle strain and (peak) muscle elongation velocity on the probability of the occurrence of a hamstring strain injury. Beside peak muscle strain and peak muscle elongation velocity, muscle fiber lengths and pennation angles also need to be considered when determining the relative risk for strain injuries among the hamstring muscles (Best et al., 1995; Thelen et al., 2005). It is also important to recognize that muscle- tendon lengthening is not necessarily linearly related to muscle fiber strain because of the interactions between tendon elasticity and muscle contraction during movements (Zajac, 1989). Finally, it is recommended that future work is needed regarding optimization of the Smart Sensor Shorts. As limitations regarding the development of the methodology are caused partly by the hardware modules. Software limitations are mainly caused by the filter parameter(s) of the sensor fusion algorithm, as these need to be optimized for this particular objective.

In conclusion, although the injury mechanism of a hamstring strain injury have been examined extensively, the current knowledge regarding the influences of muscle strain and muscle elongation velocity on the injury mechanism is limited. This study adds to the current knowledge by providing a comprehensive methodology to estimate joint kinematics, muscle strains and muscle elongation velocities with the use of IMUs. The methodology could be used in the assessment of hamstring strain injuries in professional and recreational football athletes.

ACKNOWLEDGMENT

We are grateful to MSc Linda Plaude for help with the designing of the Smart Sensor Shorts, to MSc Erik Wilmes and Jasper van Zon for help with the data analysis and we also want to thank all participants for helping out during the measurements. This study was supported by the KNVB (Zeist) and the BioMechanical Engineering department of the TU Delft for which we want to express our gratitude.

REFERENCES

- [1] Arnold, A. S., Salinas, S., Hakawa, D. J., & Delp, S. L. (2000). Accuracy of muscle moment arms estimated from MRI-based musculoskeletal models of the lower extremity. *Computer Aided Surgery*, 5(2), 108-119.
- [2] Barnes, C., Archer, D., Bush, M., Hogg, R., & Bradley, P. (2014). The evolution of physical and technical performance parameters in the English Premier League. *International Journal of Sports Medicine*, 35, 1-6.
- [3] Best, T. M., McElhaney, J. H., Garrett, W. E., & Myers, B. S. (1995). Axial strain measurements in skeletal muscle at various strain rates. *Journal of biomechanical engineering*, 117(3), 262-265.
- [4] Blair, S., Duthie, G., Robertson, S., Hopkins, W., & Ball, K. (2018). Concurrent validation of an inertial measurement system to quantify kicking biomechanics in four football codes. *Journal of biomechanics*, 73, 24-32.
- [5] Buford, W. L., Ivey, F. M., Malone, J. D., Patterson, R. M., Pearce, G. L., Nguyen, D. K., & Stewart, A. A. (1997). Muscle balance at the knee-moment arms for the normal knee and the ACL-minus knee. *IEEE Transactions on Rehabilitation Engineering*, 5(4), 367-379.
- [6] Chappell, J. D., & Limpisvasti, O. (2008). Effect of a neuromuscular training program on the kinetics and kinematics of jumping tasks. *The American journal of sports medicine*, 36(6), 1081-1086.
- [7] Chumanov, E. S., Heiderscheidt, B. C., & Thelen, D. G. (2007). The effect of speed and influence of individual muscles on hamstring mechanics during the swing phase of sprinting. *Journal of biomechanics*, 40(16), 3555-3562.
- [8] Chumanov, E. S., Heiderscheidt, B. C., & Thelen, D. G. (2011). Hamstring musculotendon dynamics during stance and swing phases of high speed running. *Medicine and science in sports and exercise*, 43(3), 525.
- [9] DeProft, E., Clarys, J. P., Bollens, E., Cabri, J., & Dufour, W. (1988). Muscle activity in the soccer kick. Reilly T, Lees A, Davis K, 16.
- [10] Giagazoglou, P., Katis, A., Kellis, E., & Natsikas, C. (2011). Differences in soccer kick kinematics between blind players and controls. *Adapted Physical Activity Quarterly*, 28(3), 251-266.
- [11] Heiderscheidt, B. C., Hoerth, D. M., Chumanov, E. S., Swanson, S. C., Thelen, B. J., & Thelen, D. G. (2005). Identifying the time of occurrence of a hamstring strain injury during treadmill running: a case study. *Clinical Biomechanics*, 20(10), 1072-1078.
- [12] Herzog, W., & Read, L. J. (1993). Lines of action and moment arms of the major force-carrying structures crossing the human knee joint. *Journal of anatomy*, 182(Pt 2), 213.
- [13] Inoue, K., Nunome, H., Sterzing, T., Shinkai, H., & Ikegami, Y. (2014). Dynamics of the support leg in soccer instep kicking. *Journal of sports sciences*, 32(11), 1023-1032.
- [14] Kellis, E., & Katis, A. (2007). Biomechanical characteristics and determinants of instep soccer kick. *Journal of sports science & medicine*, 6(2), 154.
- [15] Lieber, R. L., & Friden, J. (1993). Muscle damage is not a function of muscle force but active muscle strain. *Journal of Applied Physiology*, 74(2), 520-526.
- [16] Luinge, H. J., Veltink, P. H., & Baten, C. T. (2007). Ambulatory measurement of arm orientation. *Journal of biomechanics*, 40(1), 78-85.
- [17] Németh, G., & Ohlsén, H. (1985). In vivo moment arm lengths for hip extensor muscles at different angles of hip flexion. *Journal of biomechanics*, 18(2), 129-140.
- [18] Opar, D. A., Williams, M. D., & Shield, A. J. (2012). Hamstring strain injuries. *Sports Medicine*, 42(3), 209-226.
- [19] Reenalda, J., Maartens, E., Homan, L., & Buurke, J. J. (2016). Continuous three dimensional analysis of running mechanics during a marathon by means of inertial magnetic measurement units to objectify changes in running mechanics. *Journal of biomechanics*, 49(14), 3362-3367.
- [20] Reenalda, J., Maartens, E., Homan, L., & Buurke, J. J. (2016). Continuous three dimensional analysis of running mechanics during a marathon by means of inertial magnetic measurement units to objectify changes in running mechanics. *Journal of biomechanics*, 49(14), 3362-3367.
- [21] Riley, P. O., Dicharry, J., Franz, J. A. S. O. N., Della Croce, U., Wilder, R. P., & Kerrigan, D. C. (2008). A kinematics and kinetic comparison of overground and treadmill running. *Medicine & Science in Sports & Exercise*, 40(6), 1093-1100.
- [22] Roetenberg, D., Luinge, H., & Slycke, P. (2009). Xsens MVN: Full 6DOF human motion tracking using miniature inertial sensors. Xsens Motion Technologies BV, Tech. Rep. 1.

- [23] Roetenberg, D., Slycke, P. J., & Veltink, P. H. (2007). Ambulatory position and orientation tracking fusing magnetic and inertial sensing. *IEEE Transactions on Biomedical Engineering*, 54(5), 883-890.
- [24] Schache, A. G., Ackland, D. C., Fok, L., Koulouris, G., & Pandy, M. G. (2013). Three-dimensional geometry of the human biceps femoris long head measured in vivo using magnetic resonance imaging. *Clinical Biomechanics*, 28(3), 278-284.
- [25] Schache, A. G., Dorn, T. W., Blanch, P. D., Brown, N. A., & Pandy, M. G. (2012). Mechanics of the human hamstring muscles during sprinting. *Medicine & science in sports & exercise*, 44(4), 647-658.
- [26] Schache, A. G., Kim, H. J., Morgan, D. L., & Pandy, M. G. (2010). Hamstring muscle forces prior to and immediately following an acute sprinting-related muscle strain injury. *Gait & posture*, 32(1), 136-140.
- [27] Schache, A. G., Wrigley, T. V., Baker, R., & Pandy, M. G. (2009). Biomechanical response to hamstring muscle strain injury. *Gait & posture*, 29(2), 332-338.
- [28] Sinclair, J. (2016). Side to side differences in hamstring muscle kinematics during maximal instep soccer kicking. *Movement & Sport Sciences-Science & Motricité*, (91), 85-92.
- [29] Stevens, T. G., de Ruyter, C. J., van Niel, C., van de Rhee, R., Beek, P. J., & Savelsbergh, G. J. (2014). Measuring acceleration and deceleration in soccer-specific movements using a local position measurement (LPM) system. *International journal of sports physiology and performance*, 9(3), 446-456.
- [30] Thelen, D. G., Chumanov, E. S., Hoerth, D. M., Best, T. M., Swanson, S. C., Li, L. L., ... & Heiderscheit, B. C. (2005). Hamstring muscle kinematics during treadmill sprinting. *Med Sci Sports Exerc*, 37(1), 108-14.
- [31] Wan, X., Qu, F., Garrett, W. E., Liu, H., & Yu, B. (2017). The effect of hamstring flexibility on peak hamstring muscle strain in sprinting. *Journal of sport and health science*, 6(3), 283-289.
- [32] Winter, D. A. (2009). *Biomechanics and motor control of human movement*. John Wiley & Sons.
- [33] Woods, C., Hawkins, R. D., Maltby, S., Hulse, M., Thomas, A., & Hodson, A. (2004). The Football Association Medical Research Programme: an audit of injuries in professional football—analysis of hamstring injuries. *British journal of sports medicine*, 38(1), 36-41.
- [34] Yu, B., Lin, C. F., & Garrett, W. E. (2006). Lower extremity biomechanics during the landing of a stop-jump task. *Clinical Biomechanics*, 21(3), 297-305.
- [35] Yu, B., Queen, R. M., Abbey, A. N., Liu, Y., Moorman, C. T., & Garrett, W. E. (2008). Hamstring muscle kinematics and activation during overground sprinting. *Journal of biomechanics*, 41(15), 3121-3126.
- [36] Zajac, F. E. (1989). Muscle and tendon: properties, models, scaling, and application to biomechanics and motor control. *Critical reviews in biomedical engineering*, 17(4), 359-411.
- [37] Zimmermann, T., Taetz, B., & Bleser, G. (2018). IMU-to-segment assignment and orientation alignment for the lower body using deep learning. *Sensors*, 18(1), 302.

AUTHORS

- ¹S.S. Vinasithamby is with the Department of BioMechanical Engineering, Faculty 3mE; Delft University of Technology, Mekelweg 2, 2628 CD Delft, The Netherlands, and with the KNVB, Woudenbergseweg 56, 3707 HX Zeist, The Netherlands.
- ²E. Wilmes is with the Department of BioMechanical Engineering, Faculty 3mE; Delft University of Technology, Mekelweg 2, 2628 CD Delft, The Netherlands, with the Department of Human Movement Sciences, Faculty of Behavioural and Movement Sciences; Vrije Universiteit Amsterdam, De Boelelaan 1105, 1081 HV Amsterdam, The Netherlands and with the KNVB, Woudenbergseweg 56, 3707 HX Zeist, The Netherlands.
- ³A.S.M. Steijlen is with the Department of Microelectronics, Faculty EWJ; Delft University of Technology, Mekelweg 2, 2628 CD Delft, The Netherlands.
- ⁴K.M.B. Jansen is with the Department of Design Engineering, Faculty IO; Delft University of Technology, Mekelweg 2, 2628 CD Delft, The Netherlands.
- ⁵E.A. Goedhart is with the KNVB, Woudenbergseweg 56, 3707 HX Zeist, The Netherlands.
- ⁶F.C.T. van der Helm is with the Department of BioMechanical Engineering, Faculty 3mE; Delft University of Technology, Mekelweg 2, 2628 CD Delft, The Netherlands.

A

Construction of the Smart Sensor Shorts

A.1. Design phase

The design of the Smart Sensor Shorts is based on the currently growing topic of discussion and an innovative application of textile; Smart Clothing. Smart clothes are traditional normal clothing items that have been enhanced with modern technology, mainly electronics. The Smart Sensor Shorts is a training tight which has been enhanced with Inertial Measurement Units (IMUs) and accessory electronica (e.g. hardware to power and communicate with the sensors).

After conducting a literature study, it has been found that five IMUs are needed to quantify the risk for sustaining a hamstring strain injury in professional and recreational football athletes. These IMUs need to be placed on the pelvis, on the left and right thigh and shank. The exact locations of these IMUs on the Smart Sensor Shorts are based on results found by Saito et al. (2018) regarding the best placement of IMUs on the thigh and shank in terms of minimization of the Root Mean Square Error between the orientation estimation of the IMUs and an Optoelectronic Motion Analysis System (the golden standard in human motion analysis). It has been concluded that the lowest RMSE in orientation estimation is found by placing IMUs related to the thigh and the shank on respectively 75% of an anthropometric measurement of the length between the hip and knee joint and 50% of an anthropometric measurement of the length between the knee and ankle joint (Fig. 1.). However as the locations regarding the frontal plane are known, the placement regarding the sagittal and transverse plane are yet to be determined.

“Soft tissue artefact (STA) results from unequal movement of soft tissue layers, including muscle, tendon and dermis, between the bone and the skin surface. STA can arise from three main sources: skin sliding relative to underlying bone, inertial effects of skin motion, and deformation caused by muscle contraction” (Fiorentino et al., 2017). To avoid influences of soft tissue artefacts, IMUs need to be placed directly on to bone surfaces. However, this is not always possible. The most optimal solution is to place the IMUs on locations with the least muscle in between the bone and the skin surface. For the current location on the thigh (75% of the length between the hip and knee joint), this is the posterior lateral side of the thigh, also named the *iliotibial tract*. Regarding the shank, the location with the least muscle in between the bone and the skin surface is at the anterior medial side of the tibia. The last IMU needs to be placed on the pelvis, as data is needed from the trunk to estimate joint angle kinematics of the hips. The only area of the tight that is contact with the trunk is the elastic band of the tight. For this reason, the IMU is attached to the centre of the rear end of the thigh which is in contact with the posterior side of the pelvis. The locations of the IMUs are measured from the form of the tight itself (Fig. 2). It is assumed that the elastic band is located at the hip joints. On the tights there are sewing seams which represent the knee. It is assumed that the centre of the sewing seams represent the centre of the knee joint and that the end of the tight legs represent the centre of the knee joint (Fig. 1).



Fig. 1

Schematic design of the first prototype of the Smart Sensor Shorts with the locations of the IMUs and accessory hardware. Where L_{H-K} is the anthropometric measurement of length hip- to knee joint, L_{K-A} stands for anthropometric measurement of length knee- to ankle joint and where CoM and CoR are the abbreviations for Centre of Mass and Centre of Rotation, respectively.



Fig. 2

The methods used to mark the locations of the IMU's. The tights are folded, where after needles are used (center and right), to assure that the locations of the left and the right leg are the same. The arrows indicate the sewing seams, from where the center of the knee joint is estimated.

A.2. Construction phase

A.2.1. Parts list

- Nike Pro Tight (Nike Inc., Beaverton, United States of America)
- Waist pack (Shoppartners B.V., Alkmaar, the Netherlands)
- MPU-9250 Nine-Axis (Gyro + Accelerometer + Compass) MEMS MotionTracking™ Device (InvenSense Inc., San Jose, United States of America)
- Arduino Due (Arduino, Somerville, United States of America)
- Prototyping Shield PCB for Arduino (Kiwi Electronics B.V., Rijswijk, the Netherlands)
- Lithium Ion Polymer Accu - 3.7v 1200mAh (Kiwi Electronics B.V., Rijswijk, the Netherlands)
- PowerBoost 500 Basic - 5V USB Boost @ 500mA of 1.8V+ (Adafruit Industries, New York City, United States of America)
- TCA9548A I2C Multiplexer (Adafruit Industries, New York City, United States of America)
- MicroSD card breakout board+ (Adafruit Industries, New York City, United States of America)
- Samsung Evo plus Micro SD 128GB (Samsung Electronics, Suwon, South Korea)

<i>Part</i>	<i>Price</i>
<i>Nike Pro Tight</i>	€ 35.00
<i>Waist pack</i>	€ 4.47
<i>MPU-9250 Nine-Axis</i>	€ 18.09
<i>Arduino Due</i>	€ 39.95
<i>Prototyping Shield PCB for Arduino</i>	€ 3.95
<i>Lithium Ion Polymer Accu</i>	€ 11.95

<i>PowerBoost 500 Basic</i>	€ 17.95
<i>I2C Multiplexer</i>	€ 7.95
<i>MicroSD card breakout board+</i>	€ 8.50
<i>Samsung Evo plus Micro SD</i>	€ 30.90
<i>total</i>	€ 178.71

Note that the price is estimated without the costs of fixation materials, e.g. sewing thread, solder tin, wires etc.

A.2.2. Sewing

Firstly, the right part of the IMU (Fig. 3) is discomposed, as this part is not necessary and to eventually reduce the size of the IMU. After the desired locations are marked, the IMUs are sewed to the tights with normal sewing thread. The IMU contains four solder holes on top, four on the bottom and three on the right side (Fig. 3). The IMU could communicate either via I²C or SPI protocol. As SPI requires more wire connections between the IMUs and the hardware which makes the Smart Sensor Shorts less robust and user friendly, I²C is chosen as communication protocol. To use I²C communication, only the four top solder holes are needed. Therefore, the other seven solder holes are used to sew the IMU on to the tights. However, due to the high temperatures that are reached during soldering, wires are firstly soldered to the four solder points before the IMUs are sewed on to the tights (Chapter A.2.3.). As high temperatures could cause the thread and the fabric of the tights to incinerate. The IMUs are connected to the hardware by coated copper wires.

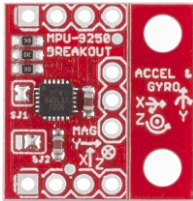


Fig. 3
The top view of a MPU- 9250 IMU with 11 solder holes.

After soldering of the wires to the IMUs, the IMUs are sewed to the tights with loose hanging wires which eventually need to be soldered to the hardware. The loose wires are then sewed on to the tight in a wave pattern (Fig. 4). This pattern and thus the wires stretches with the fabric which avoids the fracture of the wires due to tensile load, as stretching of the fabric of this type of tights is caused by stretching of the skin due to movements performed and/ or muscle contractions.



Fig. 4

An impression of the application of the wave pattern (left) and the application of the wave pattern on the tights (right).

To eventually store the hardware modules, a waist pack (without the straps) has been sewed to the elastic band of the tight (Fig. 5). Due to simplicity in storing the hardware, the wires will stick out of the pack. This means that the current zipper could not be used. Therefore, Velcro tape has been sewed on to the inside of the top “lid” of the waist pack and on to the outside of the bottom “lid” (Fig. 6). So that there is space for the wires to stick out of the waist pack and so that the waist pack could be closed.



Fig. 5

The waist pack attached to the rear end of the tight (on to the elastic band of the tight) and the attachment of Velcro tape (indicated with the arrow) on the waist pack.

A.2.3. Soldering

The first step in soldering is to solder the wires to the IMUs. During the first step, the wires are firstly hooked into the solder holes, where after they are twisted around the wire itself and eventually soldered. This creates a more stable connection that is resistant to tensile load. To avoid short circuit, heat shrink tubes are used around the end of the wires (Fig. 6).

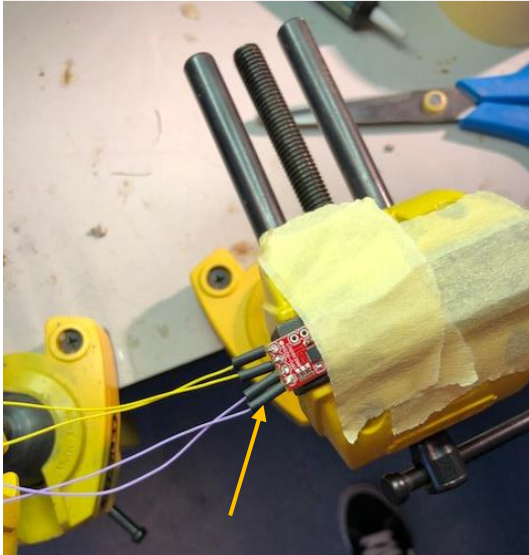


Fig. 6

Set-up during the soldering of the coated copper wires to the IMU, where after shrink tubes (indicated with the arrow) are attached to the (loose hanging) wires.

The other end of the wires need to be soldered to the hardware. The hardware consists out of multiple modules:

- Arduino Due (microprocessor)
- Prototyping Shield PCB for Arduino (expansion module Arduino Due for soldering)
- Lithium Ion Polymer Accu - 3.7v 1200mAh (power source)
- PowerBoost 500 Basic - 5V USB Boost @ 500mA of 1.8V+ (convert power from accu to a voltage needed by the different modules)
- TCA9548A I2C Multiplexer (module to communicate with multiple I²C devices)
- MicroSD card breakout board+ (module to write and read to a MicroSD card)

Firstly, the Prototyping Shield is attached to the Arduino Due with pin headers which are soldered on to the Shield. The Shield with the pin headers is “clicked” into the headers of the Arduino Due, which means that the Shield is detachable. The TCA9548A I2C Multiplexer and MicroSD card breakout board+ are soldered to the Arduino Due by soldering wires from the two modules to the Prototyping Shield PCB. These wires are larger in diameter than the wires used for soldering on to the IMUs, because these wires do not need to be flexible as they will not be sewed on the tights. Thicker wires create a more stable connection. The other end of the wires soldered to the IMUs are then soldered on to the Prototype Shield and on to the I²C Multiplexer module. The wires soldered to the power and to the ground of the IMUs are soldered to the Prototyping Shield and the wires soldered to the two I²C points (SDA and SCL) are soldered on to the I²C Multiplexer module. The power is fed to the Arduino Due via the Prototyping Shield, where after the power is fed to the individual modules (e.g. IMUs, MicroSD card breakout board+) via the Arduino Due. The power is fed to the Arduino Due via the PowerBoost 500 Basic which is connected to the Lithium Ion Polymer Accu with a JST connector. The PowerBoost 500 Basic is connected directly to the Arduino Due via a micro USB 2.0 cable. All the hardware modules are fixed to the inside of the waist pack with double sided tape (Fig. 7).

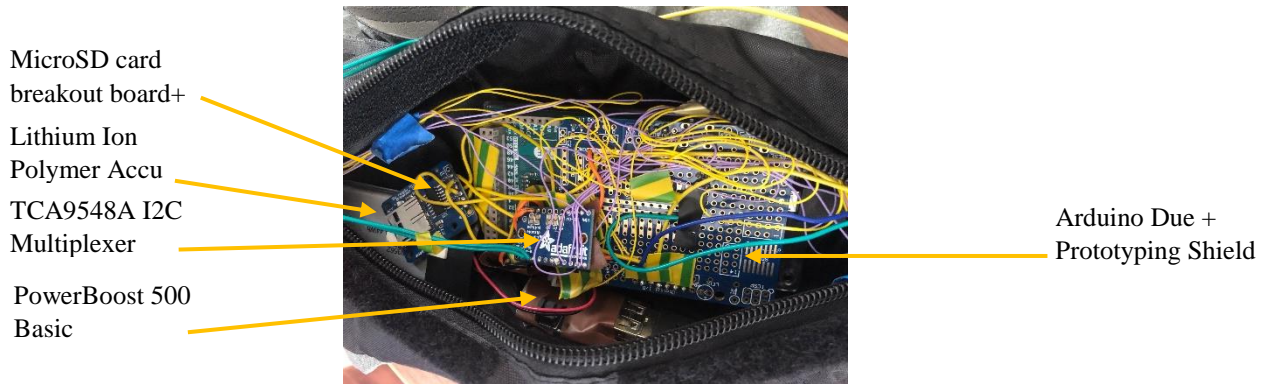


Fig. 7
The final set-up of all the hardware modules placed in the waist pack.

A.2.4. Casting

To protect the IMUs against external factors, e.g. sweat, rain, impacts and generate more robustness of the Smart Sensor Shorts, the IMUs are casted with silicone rubber (Fig. 8). For casting, one of the available silicone rubbers within the University of Technology Delft is used; “SILICONEN ADDITIE TRANSPARANT 15 NORMAAL (ZACHT)” as A component with Siliconen A Transparant FAST B Component Katalysator as B component from *Silicones and more* in the mix ratio 10:1 (A:B). This specific silicone is advised by the company for the use of casting of electronics.



Fig. 8
The IMU attached to the tights before (left) and after the casting procedure.



Fig. 9

An impression of the design of the Smart Sensor Shorts (left) and a subject wearing the constructed prototype of the Smart Sensor Shorts (with reflective markers attached to it) (center and right). The location of the five IMUs is indicated with the orange circles (center and right).

A.3. Programming phase

The programming of the Smart Sensor Shorts is done with Arduino IDE (Arduino, Somerville, United States of America) which is the programming environment to communicate with an Arduino microprocessor. The library and source code is obtained from GitHub. The communication between the IMUs and the Arduino Due is regulated by the I²C Multiplexer. This module contains five ports, each for an individual IMU. Within each sample point, the module opens each port alternately. In other words, first port 1 opens and accelerometer, gyroscope and magnetometer data from IMU one is obtained for sample point 1, then port 1 closes and port 2 opens and accelerometer, gyroscope and magnetometer data from IMU two is obtained for same sample point etc.

The biggest disadvantage of using an Arduino and this library is that the sample frequency is different each sample point and the sample frequency is limited to 165 ± 17.5 Hz. The differing sample frequency is caused by delays inside the communication of Arduino with the IMUs and the hardware modules. The data obtained from each IMU for each sample point is then written binary on to a MicroSD card in a .dat file, as binary writing results in a higher sample frequency than normal (hexadecimal) writing. Note that to eventually read the data and for the data to be used for data processing, the binary data needs to be translated to hexadecimal. This is currently done in Matlab (Mathworks, Natick, United States of America) with an algorithm, in the post processing phase.

A.4. Calibration IMUs

IMUs are relatively inexpensive, however this type of sensors suffers from inaccuracies. To minimize these inaccuracies, each IMU need to be calibrated for. As mentioned before, each IMU consist out of an accelerometer, a gyroscope and a magnetometer with each containing inaccuracies. This means that each of these three need to be calibrated separately. However, the outcome of each calibration is the same, namely a scale factor and a offset value. With these two parameters the accurate data could be estimated by;

$$data = (measurement - offset) \cdot scale\ factor$$

A.4.1. Calibration of the accelerometer

For the accelerometer, the calibration is performed by placing the IMU in the X, -X, Y, -Y, Z and -Z direction possible and measure the output of the accelerometer of the IMU. The accelerometer measures the acceleration, however in the real world gravity is always active on body's with a mass and thus also on the IMU. This means that in an "unloaded" state, the direction and magnitude of the gravitation is known and this need to be the only active acceleration measured. To eventually calibrate the accelerometer, the IMU need to be placed in the following directions "unloaded" on a flat and level surface with the;

- Y- axis upwards for 10 sec.
- Y- axis downwards for 10 sec.
- X- axis upwards for 10 sec.
- X- axis downwards for 10 sec.
- Z- axis downwards for 10 sec.
- Z- axis upwards for 10 sec.

The measurements of the accelerometer of the IMU in these six states is then post processed by an algorithm, which compares the known gravity vector to the output of the accelerometer. This algorithm then calculates the scale factor and the offset value for the X, Y and Z axis.

A.4.2. Calibration of the gyroscope

The gyroscope is more difficult to calibrate as this calibration and thus the scale factor and the offset value need to be determined by rotating the IMU through a known set of rotations and measure the output of the gyroscope. If a human would like to perform the rotations a gyro triad is need. The gyro triad is mounted in a square block and a square corner is needed to rotate against. However, as this is not available the calibration is performed in the same measurement set ups as used in the calibration of the accelerometer. As it is known that in the "unloaded" state on a flat and level surface the angular velocities are zero. By measuring the angular velocities in the directions used for the accelerometer calibration, the offset value could be determined with an algorithm. The scale factor is then estimated by using a given sensitivity value by the manufacturer.

A.4.3. Calibration of the magnetometer

Distortions of the earth's magnetic field are a result of external magnetic influences generally classified as either hard iron or soft iron biases. The ideal response surface without distortions of the magnetometer of the IMU is a sphere centered at the origin. To achieve this, the magnetometer calibration need to correct for hard iron and soft iron biases. Hard iron distortion is produced by materials that create a constant and additive field to the Earth's magnetic field, thereby generating a constant offset value to the output of the magnetometer in the X, Y and Z direction. The hard iron biases are the largest and are corrected for with measurement data of the magnetometer during a period where the IMU is moved slowly in an figure eight pattern in every direction and orientation possible inside the measuring volume which will eventually be used for the experiments. Unlike hard iron distortions, where the magnetic field is additive and constant to the Earth's magnetic field, soft iron distortions are the result of materials that influences or distorts a magnetic field, but do not necessarily generate a magnetic field itself and is therefore not additive. Soft iron correction is performed with the use of the same measurement data of the magnetometer measured for the correction of the hard iron biases. The measurements of the magnetometer of the IMU during a period where the IMU is moved slowly in an figure eight pattern in every direction and orientation possible is then post processed by an algorithm. This algorithm uses the measurement data to generate a sphere centered at the origin by estimating and using an offset value and a scale

factor. The offset value corrects for the hard iron biases and the scale factor corrects for the soft iron biases.

B

Optimization of kinematic data

The kinematic data is estimated with the use of a sensor fusion algorithm, also known as the Madgwick filter. This filter is “an efficient orientation filter for inertial and inertial/ magnetic sensor arrays” (Madgwick, 2010). It uses a quaternion representation. The filter estimates the orientation with the use of three raw data sets measured by an Inertial Measurement Unit; the acceleration, the angular rate and the magnetic field strength. Compared with a Kalman filter, the Madgwick filter “achieves levels of accuracy exceeding that of the Kalman-based algorithm; < 0.6 deg. static RMSE, < 0.8 deg. dynamic RMSE” (Madgwick, 2010), while the Madgwick filter is computationally inexpensive, is effective at low sampling rates and contains only one adjustable filter parameter (i.e. β). The orientation is basically estimated by integrating the angular rate data to an estimation of the orientation (i.e. angle). However angular rate measurements are subject to bias instabilities, which means that initial zero readings of the gyroscope will cause drift over time. This means that integration of a data set with a drift error causes the drift error to accumulate over time.

The yaw axis is the most sensitive axis regarding this drift error. A small part of this drift error is removed by using a low-pass 4th order Butterworth filter with a cut-off frequency of 12 Hz. For correction of the remaining error which is still present after integration of the gyroscope data, the Madgwick filter plays an important role. The Madgwick filter uses the acceleration and magnetic field strength measurements to correct for this drift error. Gyroscope drift in the pitch (attitude) and roll axis could be removed by using accelerometer data in which the position of the Inertial Measurement is assessed relative to the gravity (a known variable in terms of magnitude and direction). Drift in the yaw axis could be removed by using the measurements of the magnetometer. The magnetometer provides the magnetic strength relative to the Earth’s magnetic North, i.e. the magnetometer provides a static reference towards Earth’s magnetic North. The reliability of magnetic field measurements could be influenced by large metal objects or other (metal) objects that generate a magnetic field (e.g. electronica). This could however be eliminated by performing a magnetometer calibration inside the measuring volume (Appendix A).

In conclusion, after integration of the gyroscope data towards an estimate of the orientation, gyroscope drift in the pitch and roll axis could be minimized/ eliminated by accelerometer measurements and gyroscope drift in the yaw axis could be minimized/ eliminated by the magnetometer measurements. This means that the amount of reliability in the gyroscope data needs to be defined, so that the filter knows the amount of correction that needs to be performed regarding gyroscope drift. Within the Madgwick filter, the amount of reliability is transformed into a filter parameter called the β (beta) gain which ranges from 0 to 0.5. The greater the value of the beta gain, the less the gyroscope measurements are trusted (it is assumed that there is a relatively large gyroscope drift after integration) and thus the more the drift error is corrected for with accelerometer and magnetometer data.

After the orientation of each individual Inertial Measurement Unit is estimated, joint angles could be calculated by determining the orientation of the (most) distal Inertial Measurement Unit relative to the proximal one using a Z-Y-X Cardan sequence.

B.1. IMU to Segment calibration

Sensor to segment calibration is performed in two steps. The y- axis of the Inertial Measurement Units is firstly set so that it is aligned with the gravity vector. This is done by letting the subject standstill for 10 sec. Subsequently the subject is asked to perform three calibration movements (Fig. 1.). The first movement is performed with one of the legs and is described as; from a neutral rest position, to a position where the hip and knee are extended (this position needs to be held for 2 sec.), to a position where the hip and knee are flexed and eventually back to the neutral rest position. The second movement is the same as the first movement but then for the other leg. The third and final movement is performed with the trunk and is described as; from a neutral rest position, to a position where the trunk is flexed and back to the neutral rest position. It is important that all these three movements are performed mainly in the sagittal plane. By letting the subject perform these movements, the sagittal plane of each segment is estimated, where after the local coordinate system of the Inertial Measurement Units is rotated so that the z- axis is perpendicular to the sagittal plane. As the placement of the sensors on each side (left, right and center) of the Smart Sensor Shorts is different, three different movements are performed so that three different sagittal planes could be estimated.



Fig. 1

The calibration movements in the correct sequence (from left to right). Firstly the execution of the calibration movements for the legs (top); from a neutral rest position to a position where the hip and knee are extended, to a position where the hip and knee are flexed and eventually back to the neutral rest position. Lastly the execution of the calibration movement for the pelvis (bottom); from a neutral rest position, to a position where the trunk is flexed and back to the neutral position.

B.2. β gain

To eventually optimize the kinematic data estimated by the Madgwick filter, the filter parameter β needs to be tuned. Optimization is done by minimizing the Root Mean Squared Error (RMSE) between the kinematic data (i.e. joint angles and joint angular velocities) estimated by the Madgwick filter with the use of the Smart Sensor Shorts and the kinematic data estimated by an Optoelectronic Motion Analysis System (VICON Nexus). It is assumed that the kinematic data obtained with Optoelectronic Motion Analysis System is the golden standard and is thus used as the reference. As mentioned above, β describes the reliability in the gyroscope. It is assumed that β depends on the movement performed. As more dynamic movement results in greater values of angular rate. The higher the angular rates during a movement, the higher the probability for inaccuracies in the measurements. In the “current”

literature, there are no studies found which optimized this filter parameter for specific movements.

For each football- specific movement (on maximal intensity) performed in the validation study (Appendix C.), the mean RMSE of the joint angles (mean over the RMSE of the left hip-, left knee-, right hip- and right knee joint angle) is assessed for four different values of β ($\beta = 0.031, 0.041, 0.063, 0.083$) which are found in the literature (Madgwick et al., 2010; Madgwick et al., 2011).

Table 1. The mean RMSE (degrees) across eight subjects and one repetition of the left and right knee flexion/ extension angle and the left and right hip flexion/ extension angle regarding the concurrent validity of the Smart Sensor Shorts compared with an Optoelectronic Motion Analysis System during a 10m sprinting, kicking and jumping movement for different values of β for a typical subject.

RMSE (deg.)	10m sprint	kick	jump (with run up)
$\beta = 0.033$	12.63	23.35	44.61
$\beta = 0.041$	5.25	5.32	22.36
$\beta = 0.063$	5.00	4.62	4.61
$\beta = 0.083$	4.96	4.52	4.43

For a 10m sprint, kick and a jump (with run up) the lowest value for RMSE is obtained with a β equal to 0.083 (Table 1). During these movements, the angular rate (mainly of the shank and mainly during dynamic movements) are great as can be seen in the raw data measured by the gyroscope). With higher angular rates, there is a possibility of inaccuracies in the measurements. This means that the reliability in the gyroscope is less and thus there is a relatively large error which need to be corrected for with accelerometer and magnetometer data.

Note that the optimization of the kinematic data is performed by assessing the RMSE for only four different fixed β values. As it is possible that the optimal value of β , which could range from 0 to 0.5, is different than the four mentioned. Another possibility is that the optimal “value” of β is dynamic/ adjustable and is a type of function that depends on the raw measurement values of the gyroscope and/ or accelerometer and thus needs to be estimated at each sample point. Further research is needed to fully optimize this filter parameter for each of the different football specific movements.



Concurrent validation internship report

C.1. Introduction

"Muscle injuries constitute more than a third of all time-loss injuries in football and field hockey and cause more than a quarter of the total injury absence, with the hamstrings and adductors being the most frequently involved (Ekstrand et al., 2016). Despite diverse efforts on prevention of muscle injuries, there is an annual increase of hamstring injuries in professional football. An important reason for this type of injuries is the high muscle stress during explosive actions like sprinting, directional changes, jumping and kicking in modern game-play (Barnes et al., 2014). However, the currently available monitoring systems are not able to measure the load of the musculoskeletal system around the hip" (Adapted from project plan P6). For this reason a new monitoring system is developed, the Smart Sensor Shorts. This system contains five Inertial Measurement Units placed on different locations on the lower extremity.

An Inertial Measurement Unit consists out of three individual sensors; accelerometer, gyroscope and magnetometer which measures respectively the acceleration, angular velocity and magnetic field in three different directions with respect to a body segment (Roetenberg et al., 2007; Roetenberg et al., 2013). Through algorithms the orientation of each segment in space could be estimated (Roetenberg et al., 2013). With the use of sensor fusion algorithms (an algorithm that combines the three raw data sets of the individual sensors) and a biomechanical model kinematics could be estimated (Roetenberg et al., 2013).

Optoelectronic Motion Analysis Systems are used in human motion and biomechanical research to estimate kinematic data (Giagazoglou et al., 2011; Inoue et al., 2014). Retroreflective markers are placed on different anatomical locations depending on the body segments of interest. The Optoelectronic Motion Analysis System tracks these markers with the use of infrared camera's through a calibrated space, to provide position data of these markers over time. Where after, this raw position data is used to estimate kinematics. Optoelectronic Motion Analysis Systems are the golden standard regarding human motion analysis and in biomechanical research, due to the fact that they provide an accurate estimate of kinematics. However, they have some limitations; limited portability, require complex set-ups, are constrained to small test areas and to mainly laboratory settings due to complex set-ups and sensitivity regarding light and reflections.

Inertial Measurement Units have already been used to estimate kinematics during sport-specific movements in different sports e.g. running (Reenalda et al., 2016), kicking (Blair et al., 2018). This indicates that there exists a possibility that Inertial Measurement Units could be used to accurately estimate human motion kinematics to substitute the Optoelectronic Motion Analysis Systems to perform sport-specific measurements on the playing field (outdoor). A combination of multiple Inertial Measurement Units attached to different body segments of interest (the Smart Sensor Shorts) overcome the limitations of Optoelectronic Motion Analysis Systems by allowing this without the restriction of a measuring volume. However, it is not known what the validity is of the Smart Sensor Shorts compared with the golden standard, the Optoelectronic Motion Analysis System. The assignment that results

from this problem and functions as an internship for the MSc program BioMedical Engineering at the Delft University of Technology reads: "Conduct a research regarding the concurrent validity of the Smart Sensor Shorts for estimating lower limb kinematic data compared with an Optoelectronic Motion Analysis System during football specific movements".

The objective of this report is thus to compare the validity of the Smart Sensor Shorts with an Optoelectronic Motion Analysis System regarding lower limb kinematic data in (recreational) athletes.

Based on the objective, a research question has been formulated, which will be answered gradually in the course of this report. This research question reads: "Could we estimate the concurrent validity of the Smart Sensor Shorts compared with an Optoelectronic Motion Analysis System in terms of Root Mean Square Error of lower limb kinematics?".

For the writing of this report, research is conducted on Inertial Measurement Units, Optoelectronic Motion Analysis Systems, concurrent validity and other matters relating to this subject. This information is obtained through research papers, books, test models (desk research).

This report is structured as follows: In the first chapter the internship location is described. Subsequently, in chapter two, the method is defined regarding concurrent validity. Within chapter three, the results are presented. Subsequently, the results are discussed and compared to the current literature. Finally, a conclusion is drawn and a recommendation has been issued regarding the concurrent validity and the internship location.

C.2. KNVB Sport Medisch Centrum

The Sport Medical Center (SMC) of the KNVB (Royal Dutch Football Association), located in Zeist at Woudenbergseweg, is a sports center where recreational athletes, professional football players and even football referees could go for a professional sports medical examination and/ or a treatment or rehabilitation of a sports injury. Since 2010, the KNVB SMC is named an FIFA Medical Centre of Excellence. Besides, the SMC is acknowledged by the Federation of Sports Medicine Organisations (FSMI) and certified by insurance companies. Within the SMC there are four different disciplines:

- *Injury consultations*
The sports doctor asks a number of questions about the complaints in a consultation and then conducts an examination of the joints, muscles and tendons. If necessary, additional research is performed such as ultrasound.
- *Sports Physiotherapy and Rehabilitation*
The physiotherapists are specialized in the treatment of acute or chronic injuries to muscles, tendons, joints and ligaments that have arisen during or through exercise. The physical therapists have experience especially with injuries that are common in football (e.g. hamstring strain injury, ACL injury).
- *Sports Medical Examination*
The doctor can assess the individual health and the capability for sports practices by conducting a sports medical examination. Besides, they could also give advice on which measures could be taken to prevent new injuries when there are existing complaints of muscles, tendons and joints.
- *Concussion Outpatient Clinic*
Scientific research regarding concussions in sports. Athletes with persistent complaints after a sustained concussions can go to the outpatient clinic for medical

supervision and treatment. The athlete will undergo multiple tests and the gathered data will be used for scientific research (with permission of the athlete) regarding the recognition of various types of concussions.

With their expertise, the sports doctors and physiotherapists also provide the sports medical supervision of the national football teams.

The center, located on the KNVB Campus, has access to extensive and advanced testing and rehabilitation facilities, including a rehabilitation pool, sports hall and artificial- and natural grass pitches. Within the SMC, the following testing and rehabilitation facilities are available:

- *DynSTABLE*
An innovative therapy and rehabilitation tool that uses a moving platform and an immersive environment to help neurological patients recover their dynamic stability and balance control.
- *Biodex System*
An automated application for constant speed isokinetic testing and/ or measurement of muscle force, joint torque and/ or power (at constant angular velocities). The system is used in the evaluation and training of the muscles and joints, mainly for the hamstring- and quadriceps muscles (knee joint).
- *VICON Nexus Motion Capture*
The athlete is equipped with reflective markers placed at different anatomical location which are of interest. Kinematics are then recorded using different motion cameras at different angles which detect the position of the reflective markers in time. Kinetics could be measured by using force plates which measures the Ground Reaction Force. Eventually kinematics and kinetics could be coupled.
- *NordBord Hamstring Testing System*
The NordBord Hamstring Testing System is the fastest, easiest and most powerful way to train, screen, monitor and rehab hamstring strength. This tool is based on the Nordic Hamstring Curl exercise.

Besides these facilities, the SMC also has a (outside) football pitch with a coupled LPM system, which makes the SMC the perfect subject testing location for biomechanical research.

C.3. Methods

C.3.1. Subjects

Eight recreational athletes (7 men, 1 women, age of 23.6 ± 2.00 years; height of 178.8 ± 9.54 cm and mass of 72.9 ± 8.40 kg) provided written informed consent to participate in this research approved by the Delft University of Technology Ethics Committee. All participants were regularly active in some type of sports.

C.3.2. Instrumentation

Participants wore the Smart Sensor Shorts, which is a Nike Pro Tight (Nike Inc., Beaverton, United States of America) integrated with five MPU-9250 Inertial Measurement Units (IMU) (InvenSense Inc., San Jose, United States of America) and an Arduino Due (101.52×53.3 mm: 36 g), I²C Multiplexer board, MicroSD Breakout board plus MicroSD card 128 GB UHS class 3, LiPo AccuPack battery and PowerBoost 500 Basic board zipped into a waist pack ($290 \times 100 \times 60$ mm) which is attached to the rear end of the tights (Fig 1.). Each IMU (dimensions: 18×17 mm) consists out of a 3D accelerometer (range: $\pm 32g$), a 3D gyroscope

(range: $\pm 2000^\circ/\text{s}$) and a 3D magnetometer (range: $\pm 4800\mu\text{T}$). The Smart Sensor Shorts has a sample rate of 165 ± 17.5 Hz.

Concurrent validity was assessed by comparing the kinematic data estimated by the Smart Sensor Shorts with the kinematic data estimated with a 8-camera Optoelectronic Motion Analysis System (VICON Nexus, Zeist, the Netherlands). Infrared cameras were placed around an indoor testing area which mimics a football pitch and tracks the reflective markers (Fig. 1). Besides, three High Speed Cameras were placed at different locations on the pitch. Twenty reflective markers (diameter: 14 mm) were attached to the outside of the Smart Sensor Shorts and on the subjects body with double sided tape and sports tape. Anatomical markers were placed on the left and right anterior superior iliac spine, left and right posterior superior iliac spine, lower lateral and posterior 1/3 surface of the left and right thigh, medial and lateral flexion-extension axis of the left and right knee, lower lateral and posterior 1/3 surface of the left and right shank and the medial and lateral malleolus along an imaginary line that passes through the trans malleolar axis (Fig. 1). To scale the VICON Nexus biomechanical model, anthropometric measures were collected from each participant (mm); body height and leg length.

Multiple calibration procedures were performed for each system. For calibration of the Motion Analysis System, the subject is asked to stand in a T- pose (static calibration) and to perform a knee extension/ flexion, hip extension/ flexion and hip abduction/ adduction for each leg (Range of Motion calibration). The Smart Sensor Shorts are calibrated by firstly letting the subject stand still in a neutral position for 20 sec. Where after, sensor to segment calibration is performed by letting the subject execute a specific movement for each segment. For the left and right leg this movement is; from a neutral position to an extended hip and extended knee position to an flexed hip and flexed knee position back to the neutral position. For the pelvis this calibration movement is; from a neutral position to a flexed trunk position back to the neutral position. All three movements need to be performed in the sagittal plane. Both systems were automatically time-synchronized and offset corrected in Matlab (Mathworks, Natick, United States of America). No magnetic disturbances were reported in the testing environment.

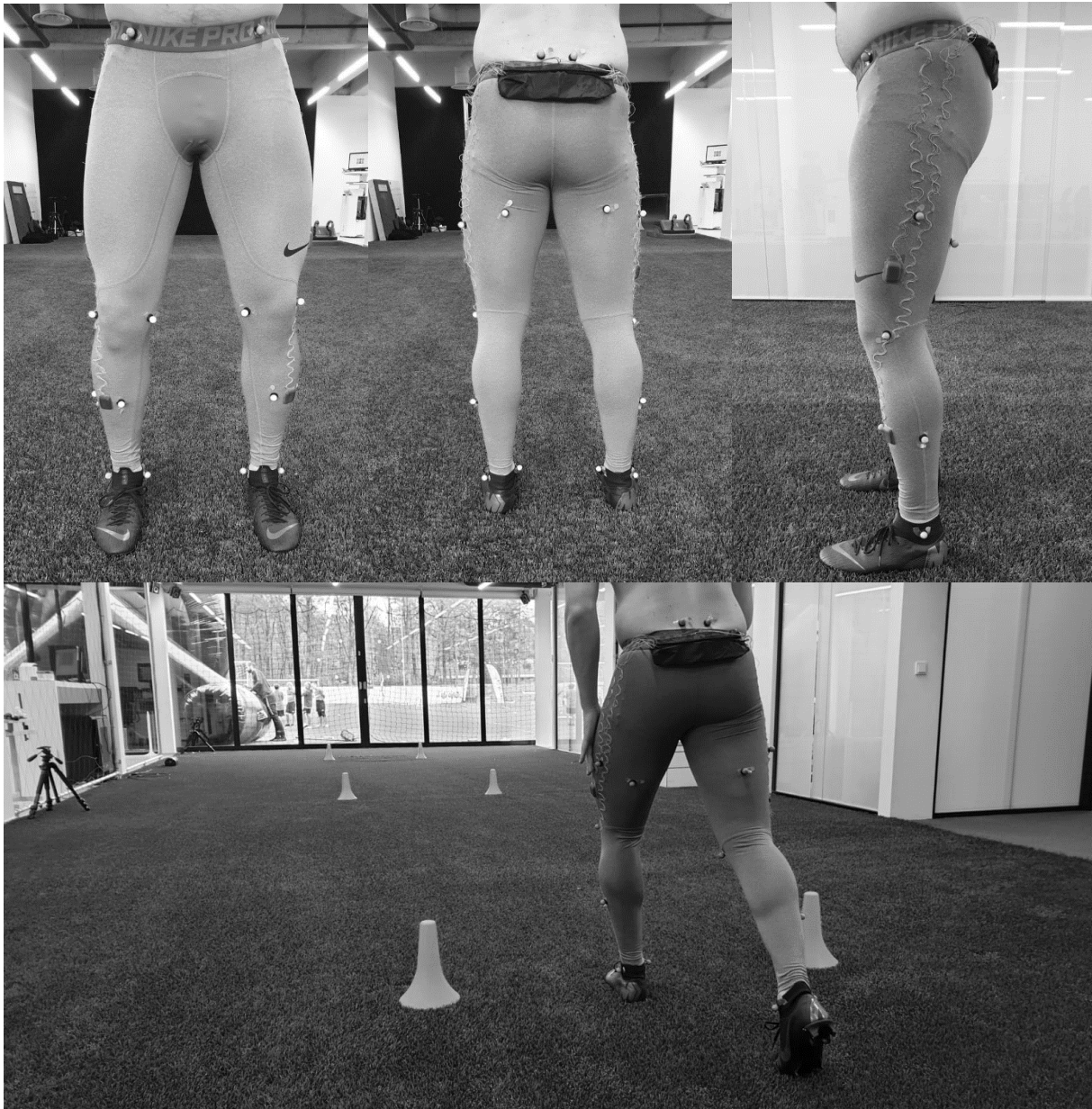


Fig. 1
The experimental test set- up used in this study. The indoor test area (top) and a subject wearing the Smart Sensor Shorts with the reflective markers attached (bottom).

C.3.3. Testing protocol

All subjects wore either (outdoor) football shoes with studs or running shoes. After attaching the reflective markers on the subject, the subject was asked to do multiple warm- up sprints on their own preference. Where after, the subjects were instructed to perform three different football specific movements (i.e. 10m sprint, kick and jump) on two intensities (i.e. “jog” and “maximal”). For the kick and the jump these intensities were respectively a football pass, a jump from standstill (“jog”) and a shot, a jump with a small run up (“maximal”). These movements are chosen as they describe the different type of individual movements which occur in football.

C.3.4. Data analysis

Data analysis was performed in Matlab (Mathworks, Natick, United States of America) for both kinematic data sets (i.e. Motion Analysis System and Smart Sensor Shorts). Raw accelerometer and gyroscope data were filtered using a low-pass 4th order Butterworth filter (cut-off frequency: 12 Hz). Type of filter and cut-off frequency were chosen based on findings in the current literature (Blair et al., 2018; Winter, 2009). Orientation estimation regarding the Smart Sensor Short were made by using an sensor fusion algorithm (Madgwick Filter) originally written by MSc E. Wilmes. Raw marker position data were filtered using a pipeline function inside VICON Nexus. Four kinematic parameters were chosen as important to hamstring strain injuries in football. These are the left and right knee flexion/ extension angle and the left and right hip flexion/ extension angle. To compare kinematic data from the Smart Sensor Shorts to the Motion Analysis System, firstly both data sets need to be time-synchronized. This is automatically done by correlation estimation. Due to the difference between both systems in local coordinate systems (of each segment), the Optoelectronic Motion Analysis System data set needs to be offset corrected for. This offset correction is performed by estimation of the mean difference between both kinematic data sets, where after the Optoelectronic Motion Analysis System data set is corrected for with a offset value. Due to technical problems (hardware failure), data of the kicking and jumping movements of one subject (age of 23 years, height of 191 cm and mass of 80 kg) could not be collected and thus not analyzed.

C.4. Results

The measurement errors in terms of Root Mean Squared (RMSE) ranged from 2.79 to 7.37 deg. for the knee- and hip flexion/ extension joint angle across three different movements for the left and right leg (table 1). These errors were classified as most likely trivia. Knee- and hip joint angles obtained from the Smart Sensor Shorts and from the Optoelectronic Motion Analysis System for the three football specific movements on two intensities for a typical subject were presented in Fig. 2.

The RMSE increases as the intensity increases of the different movements for all kinematic parameters. As for the 10m sprinting movement, a mean running speed of 2.90 ± 0.59 m/s was obtained during “jog” and a mean running speed of 4.92 ± 0.82 m/s was reached during “maximal”. The intensity difference during kicking is found in the increase in angular velocity of the knee in the kicking leg; angular velocity from 823.99 ± 5.55 to 1665.37 ± 313.96 deg./s in subject who kicked with the left leg and an increase of 1057.13 ± 350.78 to 1653.61 ± 215.10 deg./s for the angular velocity in the right leg for subjects who kicked with the right leg. For jumping the intensity difference is found in the increase of velocity in the height direction (z- axis). During jump 1 a mean speed of 2.55 ± 0.22 m/s is reached and during jump 2 a mean speed of 2.79 ± 0.31 m/s is achieved. The mean running speed and speed in the z- direction is estimated from the raw IMU data on the pelvis.

The highest RMSE in concurrent validity was observed in the left hip flexion/ extension joint angle followed by the right hip flexion/ extension joint angle averaged over all movements.

Table 1:

The mean RMSE \pm STD (degrees) of the left and right knee flexion/ extension angle and angular velocity and the left and right hip flexion/ extension angle and angular velocity regarding the concurrent validity of the Smart Sensor Shorts compared with an Optoelectronic Motion Analysis System during a 10m sprinting, kicking and jumping movement.

RMSE	left		right		left		right	
	Hip flexion/extension (deg.)	Knee flexion/extension (deg.)	Hip flexion/extension (deg.)	Knee flexion/extension (deg.)	Hip angular velocity (deg./s)	Knee angular velocity (deg./s)	Hip angular velocity (deg./s)	Knee angular velocity (deg./s)
Sprint 1	3.91 \pm 0.85	5.58 \pm 1.49	4.48 \pm 2.02	5.82 \pm 1.32	63.63 \pm 15.73	155.31 \pm 41.04	67.19 \pm 17.76	157.54 \pm 41.93
Sprint 2	6.74 \pm 1.90	7.11 \pm 1.51	6.31 \pm 3.25	7.37 \pm 2.89	109.86 \pm 39.88	209.81 \pm 69.67	105.46 \pm 27.12	248.96 \pm 76.45
Kick 1	4.78 \pm 1.41	4.21 \pm 0.86	4.01 \pm 0.84	4.78 \pm 1.15	55.47 \pm 7.62	123.73 \pm 42.71	62.52 \pm 8.02	145.93 \pm 45.45
Kick 2	7.35 \pm 3.47	5.40 \pm 2.17	6.98 \pm 3.38	4.85 \pm 0.96	89.45 \pm 17.44	181.39 \pm 68.67	94.70 \pm 22.08	205.97 \pm 68.95
Jump 1	4.85 \pm 1.70	2.79 \pm 0.68	4.32 \pm 1.36	3.49 \pm 1.29	53.60 \pm 8.42	87.21 \pm 13.97	55.65 \pm 15.75	88.24 \pm 15.83
Jump 2	6.33 \pm 1.64	5.30 \pm 1.01	5.86 \pm 1.53	5.21 \pm 1.01	60.60 \pm 12.01	118.16 \pm 28.98	65.01 \pm 15.32	119.88 \pm 28.66

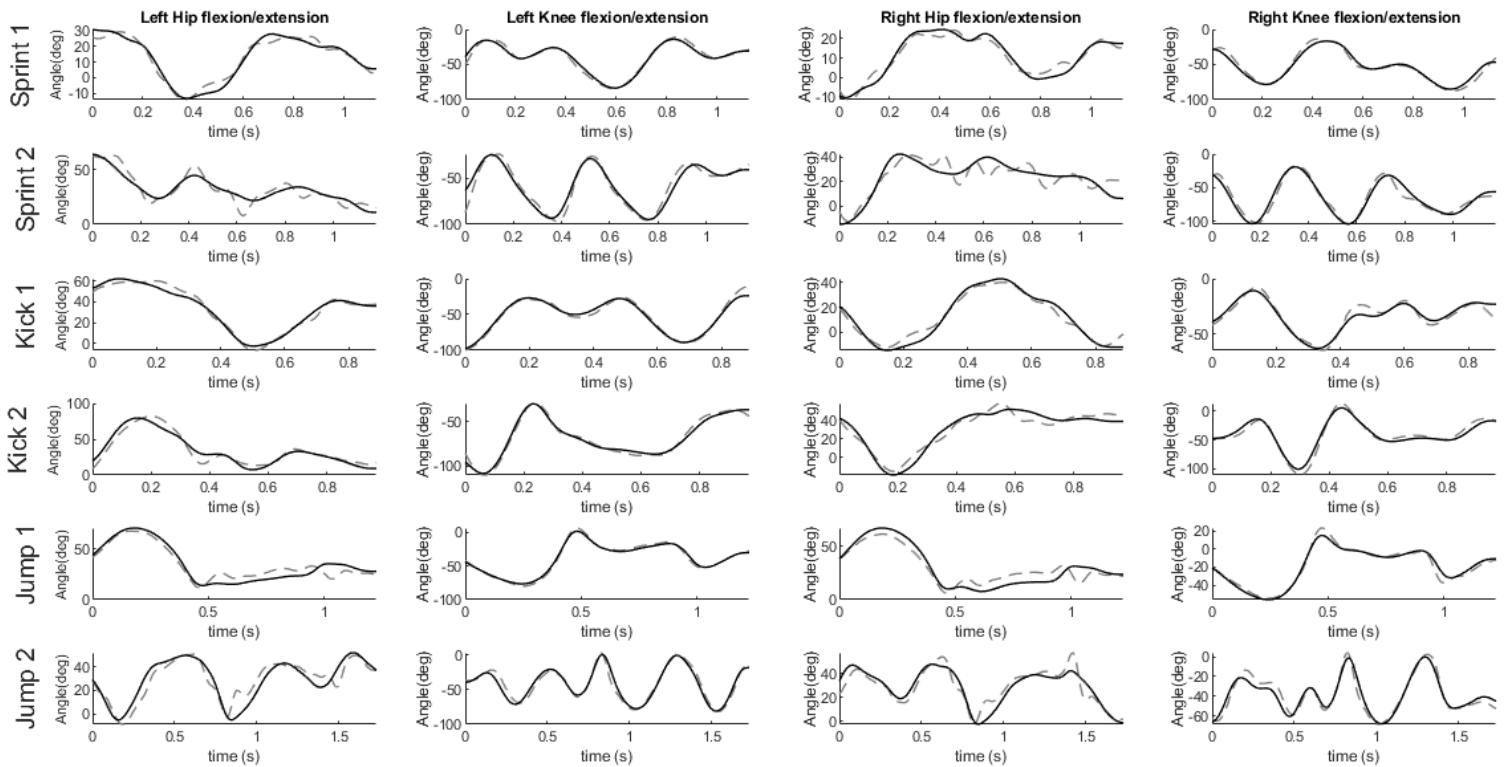


Fig. 2

Knee- and hip joint angles (in degrees) obtained from the Smart Sensor Shorts in dashed grey and from the Optoelectronic Motion Analysis System (VICON Nexus) in solid black during a 10m sprinting, kicking and jumping movement of one subject. In the plot, sprint 1 stands for jog, sprint 2 for a maximal sprint, kick 1 for a pass, kick 2 for a shot, jump 1 for a jump from standstill and jump 2 for a jump with run-up.

C.5. Discussion

The objective of this study was to investigate the concurrent validity of lower limb kinematics measured by the Smart Sensor Shorts compared to an Optoelectronic Motion Analysis System during three football specific movements. Results demonstrated that the Smart Sensor Shorts has a good concurrent validity compared to an Optoelectronic Motion Analysis System for measuring football kinematics/ biomechanics. Both measurement systems produced similar results in terms of joint angles. It is observed that the RMSE increases with intensity, as the running speed and angular velocities increases which eventually results in inaccuracies.

Besides, the RMSE is the highest in the left hip flexion/ extension joint angle followed by the right hip flexion/ extension angle. This is due to the fact that in the hip, lower values for joint angles are obtained during these specific movements than in the knee, which means that errors in the hip flexion/ action joint angle are larger in proportion. The results of this study could be compared to findings in the current literature regarding concurrent validity of lower limb kinematics between Inertial Measurement Units and Motion Analysis System. Blair et al. found better results in terms of a lower RMSE regarding sagittal knee- and hip kinematics (RMSE: 0.5 – 1.4°) during kicking in football.

The results regarding running could be compared to studies performed by respectively Cooper et al., Ferrari et al., Picerno et al., Zhang et al., which investigated the concurrent validity between the two systems for walking and running (RMSE: 0.7–3.4°, 1.6–5.2°, 0.8–3.6°, 1.8–2.4°). During the sprinting movement similar results are found in the current literature. There were no studies found in the current literature that investigated the validity between these two systems for jumping.

The differences between the results of this study and the results found in the current literature could be explained by multiple factors. The sample frequency of the Smart Sensor Shorts is lower than the sample frequency used in the studies mentioned above (i.e. Smart Sensor Shorts has 165 Hz, where Blair et al. has 1000 Hz). The higher the amount of samples, the higher the accuracy of the kinematic data. Besides, the quality of the kinematic data of the Optoelectronic Motion Analysis System depends on the set- up of the camera's and the visibility of the reflective markers in the measuring volume. It is observed that during sprinting (the subjects enters the measuring volume with speed), the reliability of the kinematic data is low due to the visibility of the markers. Further research is needed to optimize (regarding RMSE) the kinematic data obtained via the Smart Sensor Shorts by tuning multiple parameters (e.g. Madgwick filter parameters, order Butterworth filter, cut off frequency Butterworth filter) inside the orientation estimation algorithm.

The Smart Sensor Shorts offers various benefits over Motion Analysis System, e.g. easy and fast set- up and data output, outdoor testing, wide applicability regarding location and measurement range. Eventually by using the Smart Sensor Shorts instead of the golden standard, real- time feedback could be achieved which could benefit sport scientists and athletes. However, for analyses of specific movements that could be done in an laboratory/ indoor setting, the Optoelectronic Motion Analysis System is recommended due to the accuracy and reliability. Further research is needed to assess the ability of the Smart Sensor Shorts for estimating the probability of the occurrence of a hamstring strain injury in athletes.

C.6. Conclusion and recommendations

The results found in this study indicate a good concurrent validity between the Smart Sensor Shorts and the golden standard, Motion Analysis System, with small to trivial differences when measuring lower limb kinematics during football specific movements. The results are in line with results found in the current literature regarding the concurrent validity between the two systems. The observed differences could be explained by the limitations of the Smart Sensor Shorts and the test protocol in combination with the Motion Analysis System.

The results of this study evidence the use of the Smart Sensor Shorts to estimate lower limb kinematics in football.

The KNVB SMC has multiple facilities which could be used for this type of human motion/ biomechanics research. The availability of an Optoelectronic Motion Analysis System is rare in the Netherlands. Besides, the availability of an outdoor football pitch with a LPM system makes this place, a perfect location for subject testing. The close connection with sports physiotherapist (for information from another perspective) makes the KNVB SMC a perfect place regarding an MSc BioMedical Engineering/ MSc ME Biomechanical Design Internship. For these reasons, the KNVB Sport Medisch Centrum is recommended for a MSc internship. Note that students need to be able to work and to research mostly on their own, thus without direct supervision.

D

Test protocol (Dutch)

Test protocol Validatietest KNVB Smart Sensor Shorts

In te vullen door onderzoeker

Naam proefpersoon:

Dominante voet:

Test protocol Validatietest KNVB Smart Sensor Shorts

1. Smart Sensor Shorts laten aantrekken (let goed op de plaatsing van de geïntegreerde IMUs)
2. Voetbalschoenen laten aantrekken
3. Plaatsing van reflectieve markers met dubbelzijdig tape en Leukoplast tape voor stabiliteit.
4. Opmeten van de leglength
 - a. Left leglength: mm
 - b. Right leglength: mm
5. Het laten uitvoeren van (twee) oefensprintjes/ warming up (de broek naar het lichaam laten vormen en het controleren van de stabiliteit van de markers).
6. Laat de proefpersoon plaatsnemen op het krachtenplatform
7. Het uitvoeren van een statische kalibratie voor het VICON meetsysteem (handen vooruit, benen iets uit elkaar).
8. Het uitvoeren van een dynamische (ROM) kalibratie voor het VICON meetsysteem (alle mogelijke bewegingen maken met elk been).
9. Het aanzetten van de Smart Sensor Shorts
10. Laat de proefpersoon zo stil mogelijk staan voor 30 sec.
11. Controleer of de twee LEDs branden (eentje die uit het zakje steekt en eentje op het MicroSD breakout board).
12. Dubbele sprong
13. Segment to IMU kalibratie zo recht mogelijk in het sagittale vlak (linkerbeen, rechterbeen en bekken)
 - a. Hip extensie (5 sec rust)
 - b. Hip- en knie flexie
 - c. Neutrale positie
14. Dubbele sprong
15. Laat de proefpersoon lopen naar de 10m pionnen

De voetbal specifieke oefeningen

1. Dubbele sprong
2. 10 sec stilstaan
3. Sprint (10m)
 - a. Jog
 - b. Maximal
4. Rapid Stop (10m)
 - a. Jog
 - b. Maximal
5. Change of direction 180° (10m)
 - a. Jog
 - b. Maximal
6. Change of direction 45° (5m)
 - a. Jog
 - b. Maximal
7. Forward/ Backward (5m)
 - a. Jog
 - b. Maximal
8. Kick (zelf te bepalen)
 - a. Jog (pass)
 - b. Maximal (schot)
9. Jump (zelf te bepalen)
 - a. Jog (vanuit stilstand)
 - b. Maximal (met aanloop)

Note: Nadat de oefening is uitgevoerd moet er teruggelopen worden naar een aangegeven positie. De proefpersoon dient op het einde van de oefening 5 sec. stil te staan en dient na het teruglopen naar een aangegeven positie en dus voor het uitvoeren van de volgende oefening 10 sec. stil te staan.

E

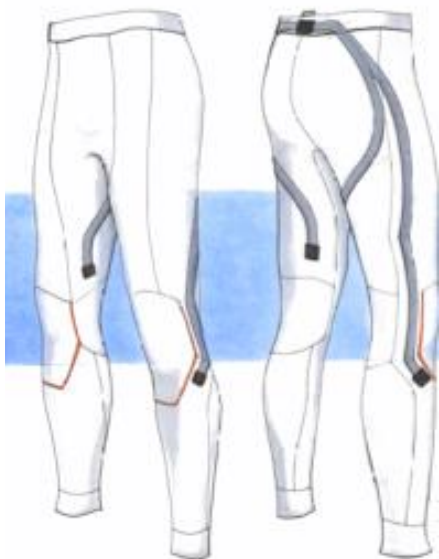
Information letter (Dutch)

Informatiebrief voor deelnemers

Voor de masteropleiding *BioMedical Engineering* aan de *Technische Universiteit Delft* doen wij onderzoek naar het voorkomen van blessures, voornamelijk in het voetbal. Daarvoor moet eerst de “Smart Sensor Shorts” (een speciaal ontworpen broek) worden gevalideerd (vergeleken met een ander meetsysteem, zodat we weten dat de broek meet wat het moet meten). Dit is een broek (in ontwikkeling) waarin sensoren zijn bevestigd die de “beweging” van spelers kan meten. Dit onderzoek vindt plaats op het Voetbal Medisch Centrum op de KNVB Campus (zie adres onderaan de pagina). Het uiteindelijke doel is om deze broek tijdens (voetbal) trainingen en -wedstrijden te kunnen gebruiken.

Het onderzoek bestaat uit een aantal voetbal specifieke oefeningen (denk aan: sprinten, draaien en schieten). Voorafgaand doe je een warming-up (\pm 10 minuten) en word je bekend met de voetbal specifieke oefeningen die tijdens de meting uitgevoerd dienen te worden. Metingen zullen worden verricht met een Bewegingsanalyse- meetsysteem (VICON Nexus). Dit is een meetsysteem dat de bewegingen van oefeningen kan volgen aan de hand van reflectieve markers die op het lichaam zijn geplakt. Markers worden geplakt op het onderlichaam (op de Smart Sensor Shorts) en onderste deel van het bovenlichaam (je moet het dus niet erg vinden om de metingen te verrichten met ontbloot bovenlichaam!).

Naast reflectieve markers en de Smart Sensor Shorts zullen een aantal IMUs (kleine sensoren, zie afbeelding hieronder voor een overzicht van de plaatsing) op je lichaam worden geplakt (onder de Smart Sensor Shorts). De verkregen data uit deze sensoren en de Smart Sensor Shorts wordt uiteindelijk vergeleken met de data uit het VICON meetsysteem. De bewegingen worden daarnaast gefilmd om deze bewegingen te herkennen/ analyseren. De video's zullen niet worden verspreid.



In totaal zal het gehele onderzoek circa 1 uur duren. Houdt er rekening mee dat een aantal voetbal specifieke bewegingen op hoge intensiteit moeten worden uitgevoerd, dus zorg ervoor dat je de dag van tevoren niet teveel inspanning levert.

Wij vragen je zelf voetbalschoenen (het liefst voor op kunstgras) mee te nemen.

Het is ten alle tijden toegestaan om je af te melden, of eerder te stoppen tijdens het onderzoek. Daarvoor dien je geen reden op te geven. Er zitten geen verdere beloningen aan dit onderzoek verbonden.

Mochten er nog vragen of onduidelijkheden zijn, of wil je (vrijwillig) deelnemen aan het onderzoek, neem dan contact op met: s.s.vinasithamby@student.tudelft.nl

Adres: Woudenbergseweg 56, 3707 HX Zeist, Voetbal Medisch Centrum
Zie de [site](#) voor bereikbaarheid met Openbaar Vervoer, fiets of auto.

F

Informed Consent (Dutch)

Smart Sensor Shorts

Validatietest

Contactgegevens onderzoekers

Naam: **Suman Vinasithamby**

Email: **s.s.vinasithamby@student.tudelft.nl**

Telefoonnummer: **06-15875477**

Voorafgaand aan het invullen van dit formulier (Informed consent) is een informatiebrief rondgegaan waarin informatie over de aard, de methode, het doel, de risico's en de belasting van het project/onderzoek is beschreven en toegelicht.

Onderstaand betreft de **Informed consent** (letterlijk: geïnformeerde toestemming), met 'Ik' wordt de proefpersoon bedoeld.

Informed consent, te lezen en in te vullen door de proefpersoon

- Ik ben op een duidelijk wijze, zowel mondeling als schriftelijk, op de hoogte gesteld over de aard, de methode, het doel, de risico's en de belasting van het onderzoek. Indien dit niet volledig duidelijk was, heb ik de mogelijkheid gekregen om vragen te stellen. Mijn vragen zijn voldoende beantwoord. Ik heb bovendien voldoende tijd gehad om te beslissen of ik meedoe.
- Ik doe vrijwillig mee. Ik kan op ieder moment beslissen om toch niet mee te doen met het onderzoek of vroegtijdig te stoppen. Hiervoor hoef ik geen reden te geven.
- Ik weet dat de onderzoekers mijn gegevens kunnen inzien. De contactgegevens van deze onderzoekers staan bovenaan vermeld in de brief.
- Ik geef toestemming voor het verzamelen en gebruiken van mijn gegevens op de manier en voor de doelen die in de informatiebrief zijn vermeld. Ik weet dat mijn gegevens vertrouwelijk zullen worden behandeld en dat resultaten van het onderzoek alleen anoniem aan derden bekend zullen worden gemaakt.
- Ik begrijp dat foto- en videomateriaal of bewerking daarvan uitsluitend voor analyse en/of wetenschappelijke presentaties zal worden gebruikt.
- Ik begrijp dat gegevens, resultaten, foto- en videomateriaal of bewerking daarvan geanonimiseerd voor onderwijsdoeleinden kan worden gebruikt.
- Ik geef toestemming om mijn gegevens nog 10 jaar na dit onderzoek te bewaren.
- Ik heb de Informed consent gelezen. De inhoud van het Informed consent is mij duidelijk en ik wil meedoen aan dit onderzoek.

Handtekening:

Datum: __ / __ / __

Gegevens proefpersoon (uit te voeren door de onderzoekers)

Naam:

Lengte (cm):

Gewicht (kg):

Geslacht: M / V

Leeftijd:

In te vullen door de uitvoerende onderzoeker(s)

- Ik verklaar dat de proefpersoon volledig is geïnformeerd over het genoemde onderzoek.
- Als er tijdens het onderzoek informatie bekend wordt die de toestemming van de proefpersoon zou kunnen beïnvloeden, dan breng ik de proefpersoon daarvan tijdig op de hoogte.

Naam onderzoeker: **Suman Vinasithamby**

Handtekening:

Datum: __ / __ / __

References

- Barnes, C., Archer, D. T., Hogg, B., Bush, M., & Bradley, P. S. (2014). The evolution of physical and technical performance parameters in the English Premier League. *International Journal of Sports Medicine*, 35(13), 1095-1100.
- Blair, S., Duthie, G., Robertson, S., Hopkins, W., & Ball, K. (2018). Concurrent validation of an inertial measurement system to quantify kicking biomechanics in four football codes. *Journal of biomechanics*, 73, 24-32.
- Cooper, G., Sheret, I., McMillian, L., Siliverdis, K., Sha, N., Hodgins, D., ... & Howard, D. (2009). Inertial sensor-based knee flexion/extension angle estimation. *Journal of biomechanics*, 42(16), 2678-2685.
- Ekstrand, J., Waldén, M., & Häggglund, M. (2016). Hamstring injuries have increased by 4% annually in men's professional football, since 2001: a 13-year longitudinal analysis of the UEFA Elite Club injury study. *Br J Sports Med*, 50(12), 731-737.
- Ferrari, A., Cutti, A. G., Garofalo, P., Raggi, M., Heijboer, M., Cappello, A., & Davalli, A. (2010). First in vivo assessment of "Outwalk": a novel protocol for clinical gait analysis based on inertial and magnetic sensors. *Medical & biological engineering & computing*, 48(1), 1.
- Fiorentino, N. M., Atkins, P. R., Kutschke, M. J., Goebel, J. M., Foreman, K. B., & Anderson, A. E. (2017). Soft tissue artifact causes significant errors in the calculation of joint angles and range of motion at the hip. *Gait & posture*, 55, 184-190.
- Giagazoglou, P., Katis, A., Kellis, E., & Natsikas, C. (2011). Differences in soccer kick kinematics between blind players and controls. *Adapted Physical Activity Quarterly*, 28(3), 251-266.
- Inoue, K., Nunome, H., Sterzing, T., Shinkai, H., & Ikegami, Y. (2014). Dynamics of the support leg in soccer instep kicking. *Journal of sports sciences*, 32(11), 1023-1032.
- KNVB. (2019, april 7). *Sportmedisch Centrum*. Retrieved from KNVB: <https://www.knvb.nl/campus/sportmedisch-centrum>
- Madgwick, S. (2010). An efficient orientation filter for inertial and inertial/magnetic sensor arrays. Report x-io and University of Bristol (UK), 25, 113-118.
- Picerno, P., Cereatti, A., & Cappozzo, A. (2008). Joint kinematics estimate using wearable inertial and magnetic sensing modules. *Gait & posture*, 28(4), 588-595.
- Reenalda, J., Maartens, E., Homan, L., & Buurke, J. J. (2016). Continuous three dimensional analysis of running mechanics during a marathon by means of inertial magnetic measurement units to objectify changes in running mechanics. *Journal of biomechanics*, 49(14), 3362-3367.
- Robert-Lachaine, X., Mecheri, H., Larue, C., & Plamondon, A. (2017). Validation of inertial measurement units with an optoelectronic system for whole-body motion analysis. *Medical & biological engineering & computing*, 55(4), 609-619.

Roetenberg, D., Luinge, H., & Slycke, P. (2009). Xsens MVN: Full 6DOF human motion tracking using miniature inertial sensors. Xsens Motion Technologies BV, Tech. Rep, 1.

Roetenberg, D., Slycke, P. J., & Veltink, P. H. (2007). Ambulatory position and orientation tracking fusing magnetic and inertial sensing. *IEEE Transactions on Biomedical Engineering*, 54(5), 883-890.

Saito, A., Miyawak, K., Komats, A., & Takemi, S. (2018). Examination of motion sensor attachment position to thigh and lower leg in gait measurement (focusing on knee joint angle in sagittal plane). *Transactions of the Japan Society of Mechanical Engineers*, 84 (865), 18-00263.

Saito, A., Miyawaki, K., Kizawa, S., & Kobayashi, Y. (2018). A study on estimating the knee joint angle during walking using the motion sensors (Focusing on the effect of centrifugal acceleration and tangential acceleration). *Transactions of the JSME (in Japanese)*, 84(857).

Winter, D. A. (2009). *Biomechanics and motor control of human movement*. John Wiley & Sons.

Zhang, J. T., Novak, A. C., Brouwer, B., & Li, Q. (2013). Concurrent validation of Xsens MVN measurement of lower limb joint angular kinematics. *Physiological measurement*, 34(8), N63.